FHL1 is a major host factor for chikungunya virus infection

Laurent Meertens, Mohamed Lamine Hafirassou, Thérèse Couderc, Lucie Bonnet-Madin, Vasiliya Kril, Beate Mareike Kümmerer, Athena Labeau, Alexis Brugier, Etienne Simon-Loriere, Julien Burlaud-Gaillard, et al.

FHL1 is a major host factor for chikungunya virus infection

Laurent Meertens[1#*], Mohamed Lamine Hafirassou[1], Therese Couderc[2], Lucie Bonnet-Madin[1], Vasiliya Kril[1], Beate M. Kümmerer[3], Athena Labeau[1], Alexis Brugier[1], Etienne Simon-Loriere[4], Julien Burlaud-Gaillard[5], Cécile Doyen[6], Laura Pezzi[7], Thibaud Goupil[2], Sophia Rafasse[2], Pierre-Olivier Vidalain[8], Anne Bertrand Legout[9], Lucie Gueneau[9], Raul Juntas-Morales[10], Rabah Ben Yaou[9], Gisèle Bonne[9], Xavier de Lamballerie[7], Monsef Benkirane[6], Philippe Roingeard[5], Constance Delaugerre[1,11], Marc Lecuit[2,12] and Ali Amara[1#*]

[1] Cell Biology of Virus Infection Team, INSERM U944, CNRS UMR 7212, Institut de Recherche Saint-Louis, Université de Paris, Hôpital Saint-Louis, 75010 Paris, France

[2] Biology of Infection Unit, Institut Pasteur, Inserm U1117, Paris, France

[3] Institute of Virology, University of Bonn Medical Centre, Bonn, Germany

[4] G5 Evolutionary Genomics of RNA Viruses, Institut Pasteur, 28 rue du Dr Roux, 75724 Paris, France

[5] INSERM U1259 MAVIVH et Plateforme IBiSA de Microscopie Electronique, Université de Tours, France

[6] Institut de Génétique Humaine, Laboratoire de Virologie Moléculaire, CNRS-Université de Montpellier, 34000 Montpellier, France

[7] Unité des Virus Émergents, Aix-Marseille Univ–IRD190–Inserm 1207 EFS-IRBA, 13005 Marseille cedex 05, France

[8] Equipe Chimie & Biologie, Modélisation et Immunologie pour la Thérapie, Université Paris Descartes, CNRS UMR 8601, Paris, France

[9] Sorbonne Université, INSERM UMRS974, Center of Research in Myology, F-75013 Paris, France.

[10] Département de Neurologie, Centre Hospitalier Universitaire de Montpellier, Montpellier, France.

[11] Laboratoire de Virologie et Département des Maladies Infectieuses, Hôpital Saint-Louis, APHP, 75010 Paris, France

[12] Université de Paris, Department of Infectious Diseases and Tropical Medicine, Necker-Enfants Malades University Hospital, APHP, Institut Imagine, Paris, France

[#] Contributed equally to the work

* Corresponding authors: ali.amara@inserm.fr; laurent.meertens@inserm.fr

ABSTRACT

Chikungunya virus (CHIKV) is a re-emerging Old World alphavirus transmitted to humans by mosquito bites which causes musculoskeletal and joint pain[1–3]. Despite intensive investigations, the identity of the human cellular factors critical for CHIKV infection remains elusive, hampering both the understanding of viral pathogenesis and the development of anti-CHIKV therapies. Here, we identified the Four-and-a-Half LIM domain protein 1 (FHL1)[4] as a host factor required for CHIKV permissiveness and pathogenesis. Ablation of FHL1 expression results in massive inhibition of infection by several CHIKV strains and O'nyong-nyong virus, but not by other alphaviruses or flaviviruses. Conversely, expression of FHL1 enhances infection of cells that do not express it and are poorly susceptible to CHIKV. We show that FHL1 directly interacts with the hypervariable domain of CHIKV nsP3 protein and is essential for viral RNA replication. FHL1 is highly expressed in CHIKV target cells and particularly abundant in muscles[4,5]. Significantly, dermal fibroblasts and muscle cells derived from Emery-Dreifuss muscular dystrophy (EDMD) patients which lack functional FHL1[6] are resistant to CHIKV infection. Importantly, CHIKV infection is undetectable in mice knocked out for the FHL1 gene. Overall, this study shows that FHL1 is a key host dependency factor for CHIKV infection and identifies nsP3-FHL1 interaction as a promising target for the development of anti-CHIKV therapies.

MAIN TEXT

Several host factors implicated in CHIKV infection have been identified, however none of them accounts for CHIKV tropism for joint and muscle tissues[7–10]. To identify key host factors dictating CHIKV cell permissiveness, we performed a genome-wide CRISPR-Cas9 screen in the HAP1 haploid cell line (Fig.1a, Extended Data Fig. 1). HAP1 cells expressing the human GeCKO v2 single guide RNA libraries A and B, which contains each 3 unique sgRNAs targeting 19,050 genes[11], were inoculated with CHIKV21, a strain isolated from a patient infected during the 2005-2006 CHIKV outbreak in La Reunion Island[12]. Genomic DNA from lentivirus-transduced cells that survived to CHIKV infection was isolated, amplified and the corresponding integrated sgRNA sequenced. Gene enrichment was assessed using the MAGeCK software[13] (Fig.1a, Extended Data Fig. 1, supplementary Table 1). The top hit of our screen was the gene encoding the Four-and-a-Half LIM protein 1 (FHL1) (Fig.1a, Extended Data Fig. 2a-c), the founding member of the FHL protein family[14]. FHL1 is characterized by the presence of four and a half highly conserved LIM domains with two zinc fingers arranged in tandem[14]. FHL1 is strongly expressed in skeletal muscles and heart[4,14]. In human, there are three FHL1 splice variants: FHL1A, FHL1B and FHL1C[4,15,16]. FHL1A is the most abundantly expressed, primarily detected in striated muscles[4] and fibroblasts[17]. The two other variants FHL1B and C are expressed in muscles, brain and testis[15,16]. We functionally validated the requirement of FHL1 in CHIKV21 infection by using two distinct gRNAs targeting all three FHL1 isoforms (Extended Data Fig. 2a). We generated HAP1 and 293T knockout *FHL1* clones (ΔFHL1) and confirmed gene editing by sequencing and western blot analysis (Extended Data Fig. 2d, e, f). FHL1 knockout did not alter cell proliferation and viability as determined by CellTiter-Glo assay (Extended Data Fig. 2g). CHIKV infection and release of infectious particles was

drastically inhibited in ΔFHL1 cells (Fig.1b, Extended Data Fig. 3a-d). Trans-complementation of ΔFHL1 cells with a human cDNA encoding FHL1A, but not FHL1B or C, restored both susceptibility to CHIKV21 infection and virus release (Fig. 1c, Extended Data Fig. 4a-b), indicating that FHL1A is a critical factor for CHIKV21 infection. Expression of FHL2, a member of the FHL family predominantly expressed in heart[18], restored CHIKV infection in ΔFHL1 cells, albeit to a lower efficiency than FHL1 (Extended Data Fig. 4c). We then assessed FHL1 dependency of CHIKV strains from distinct genotypes. FHL1 is important for infection by strains belonging to the Asian (strain St Martin H20235 2013), the ECSA (East, Central, and South African) strains Ross and Brazza (MRS1 2011) and the Indian Ocean (IOL) (strain M-899) lineages (Fig. 1d). Of note, the requirement for FHL1 was less pronounced with CHIKV 37997, a strain from the West African genotype (Fig. 1d). We next tested the requirement of FHL1 for infection by other alphaviruses. Interestingly, O'nyong-nyong virus (ONNV), an Old World alphavirus that is phylogenetically very close to CHIKV[1], showed a dramatically reduced infection level in ΔFHL1 cells (Fig.1e, Extended Data Fig. 3e). In sharp contrast, other Old World alphaviruses such as Mayaro virus (MAYV), Sindbis virus (SINV), Semliki Forest Virus (SFV) and Ross River virus (RRV), and New World encephalitic viruses such as Eastern equine encephalitis virus (EEEV), Western equine encephalitis virus (WEEV) or Venezuelan equine encephalitis virus (VEEV) infected HAP1 cells in a FHL1-independent manner (Fig. 1e, f, Extended Data Fig. 3e). No effect of FHL1 was observed for infection by Dengue virus (DENV) or Zika virus (ZIKV), two members of the *Flavivirus* genus (Fig. 1g, Extended Data Fig. 3f). Consistent with the requirement of FHL1 for CHIKV infection, BeWo or HepG2 cells which are poorly susceptible to CHIKV infection[20,21] and do not express endogenous FHL1 (Extended Data Fig. 5a) became permissive to the virus upon FHL1A expression

(Fig.1h, Extended Data Fig. 5b-d). This highlights the major role played by FHL1A in human cell permissiveness to CHIKV.

To determine which step in CHIKV life cycle requires FHL1, we challenged parental and ΔFHL1 cells with CHIKV particles and quantified the viral RNA at different time points (Fig. 2a). We did not observe any major difference in CHIKV RNA levels in FHL1-deficient cells compared to WT cells at 2h post-infection (Fig. 2a). In contrast, a massive reduction of CHIKV RNA was observed in ΔFHL1 cells as early as 6h post-infection (Fig. 2a) which was even greater 24h post-infection, suggesting that FHL1 expression is involved in an early post-entry step of the CHIKV life cycle. We therefore bypassed virus entry and uncoating by transfecting CHIKV RNA into controls or ΔFHL1 cells in the presence of NH_4Cl to inhibit further rounds of infection[9]. Upon CHIKV RNA transfection, viral replication was drastically impaired in ΔFHL1 cells compared to WT cells (Fig. 2b, Extended Data Fig 6a). To evaluate the contribution of FHL1 in incoming genome translation versus RNA replication, we generated a replication-deficient CHIKV molecular clone (with the GDD motif of the viral polymerase nsP4 mutated to GAA) encoding a *Renilla* luciferase (Rluc) fused to the nsP3 protein as described [22]. Transfection of CHIKV GAA RNA in ΔFHL1 or control cells resulted in a similar Rluc activity (Fig. 2c), indicating that FHL1 is dispensable for CHIKV incoming RNA translation. When similar experiments were performed with the WT CHIKV RNA, a massive increase in Rluc activity was observed in control cells but not ΔFHL1 24 hpi (Fig. 2d), demonstrating that FHL1 is essential for viral RNA replication. Furthermore, qRT-PCR experiments showed that ablation of FHL1 resulted in a severely reduced synthesis of CHIKV negative strand RNA (Fig. 2e). We then investigated the impact of FHL1 in the production of dsRNA intermediates which are a marker of viral replication complex (vRC) assembly[23]. At 6h post-infection, a massive reduction of dsRNA-

containing complexes was observed in ΔFHL1 cells stained with anti-dsRNA mAb when compared to parental cells (Fig. 2f). Consistent with this observation, transmission electron microscopy showed that the formation of plasma membrane-associated spherules and cytoplasmic vacuolar membrane structures, which are alphavirus-induced platforms required for viral RNA synthesis[24], are absent in ΔFHL1 cells (Fig 2g). Altogether, these data show that FHL1 is critical for CHIKV RNA replication and vRC formation in infected cells.

We next investigated FHL1 location during infection. Confocal microscopy studies showed that FHL1 displays a diffuse cytoplasmic distribution in uninfected human fibroblasts. In cells infected for 6h, FHL1-containing foci appeared and colocalized with nsP3 (Extended Data Fig. 6b), a CHIKV non-structural protein orchestrating viral replication in the cytoplasm[25,26]. Indeed, CHIKV nsP3 contains a large C-terminal hypervariable domain (HVD)[25] known to mediate assembly of protein complexes and regulate RNA amplification[25,26]. Interestingly, FHL1 and FHL2 have been reported as putative nsP3 HVD binding partners in mass spectrometry analyses [26,27]. We experimentally validated FHL1-nsP3 interaction (Fig. 2h,I; Extended Data Fig. 6c-g) and found that endogenous FHL1 co-immunoprecipitates with nsP3 from CHIKV-infected cells (Fig. 2h). Consistent with infection studies, both FHL1A and FHL2 co-precipitated with CHIKV nsP3 (Extended Data Fig. 6d). FHL1A-nsP3 interaction is specific for CHIKV as it was not observed with other alphaviruses such as SINV or SFV, which do not depend on FHL1 for infection (Extended Data Fig. 6e). Of note, in ΔFHL1 cells, nsP3 retained its ability to bind G3BP1 and 2, two components of the stress granules implicated in CHIKV replication[22,26] (Extended Data Fig. 6e). We next generated chimeric proteins where the HVD region of CHIKV nsP3 is swapped with the corresponding domain of SINV nsP3 and vice versa. Whereas CHIKV-SINV(HVD)

chimeric protein lost its ability to bind FHL1, the HVD of CHIKV in the context of SINV nsP3 protein conferred binding to FHL1 (Extended Data Fig. 6f). Pull-down experiments with purified proteins showed that FHL1A directly binds to WT nsP3 but not to the HVD-deficient variant (Fig. 2i, Extended Data Fig. 6g). We then mapped the binding region within CHIKV nsP3HVD responsible for FHL1A interaction (Fig. 2j, Extended Data Fig. 7). The FHL1 binding domain, referred as HVD-R4, is found in all CHIKV and ONNV strains and is located upstream of the short repeating peptide corresponding to G3BP1/2 binding sites[26] (Fig. 2j, Extended Data Fig. 7a). Deletion of the HVD-R4 region strongly impaired FHL1 interaction with nsP3, without affecting G3BP1/2 binding to the viral protein (Fig. 2j, Extended Data Fig. 7b). To investigate whether FHL1 interaction with the HVD region of nsP3 is required for FHL1 proviral role, we generated two chimeric FHL1A protein either fused to the HVD-R4 peptide (FHL1A-R4) or to a randomized peptide sequence of HVD-R4 (FHL1A-R4*) as a positive control (Fig. 2k, Extended Data Fig. 7c) and assessed their ability to interact with nsP3. Whereas FHL1A-R4 failed to bind nsP3 (Fig. 2k), FHL1A-R4* interacted with nsP3 as efficiently as WT FHL1A protein (Fig. 2k). These results indicate that the fused HVD-R4 peptide likely hides the binding site of FHL1A to nsP3, inhibiting their interaction. Furthermore, trans-complementation of ΔFHL1 cells with a cDNA encoding FHL1A-R4 did not restore CHIKV21 infection when compared to FHL1A-R4* or WT FHL1A (Fig. 2l). Consistent with this, *in vitro* transcribed RNA from CHIKV molecular clone mutated in FHL1 binding site (ΔR4 or R4*) showed a strong defect in replication after transfection in 293T cells (Extended Data Fig. 7d). Together these data strongly suggest that the interaction between the HVD region of nsP3 with FHL1 is critical for FHL1 proviral function.

Mutations in the *FHL1* gene have been associated with X-linked myopathies[5,28], including the Emery–Dreifuss muscular dystrophy (EDMD)[6], a rare genetic disease characterized by early joint contractures, muscular wasting and adult-onset cardiac disease[29]. We studied the permissiveness to CHIKV of dermal fibroblasts and myoblasts from four EDMD male patients carrying *FHL1* gene mutations as well as from two healthy donors (Extended Data Fig.8a). A detailed clinical description of P1, P2 and P3 has been reported[6], and patient P4 presented with EDMD and additional clinical abnormalities (see methods). Analysis of P4 *FHL1* gene revealed the insertion of a full-length LINE-1 retrotransposon sequence in exon 4 (Extended Data Fig.8b). FHL1 expression is severely reduced in primary cells from all four EDMD patients as established by immunoblot analysis (Fig. 3a). Infection studies showed that fibroblasts and myoblasts from those EDMD patients are resistant to CHIKV21 and M-899 Mauritian strains (Fig. 3b-d, Extended Data Fig.8c), and exhibit a massive defect in the release of infectious particles (Fig. 3d), in contrast to healthy donor cells. Similar results were obtained with the CHIKV strains Brazza, Ross and H20235 (Fig. 3e, Extended Data Fig.8d). FHL1-null myoblasts and fibroblasts remained highly susceptible to MAYV, which does not rely on FHL1 for replication (Fig. 3e). Trans-complementation of EDMD fibroblasts by a lentivirus encoding WT FHL1A restored CHIKV viral antigen synthesis (Fig. 3f, Extended Data Fig.8e) and infectious particle release (Fig. 3g).

To directly assess the role of FHL1 in chikungunya pathogenesis, we conducted *in vivo* experiments in mice expressing or not FHL1. Human and mouse FHL1 orthologues are highly conserved (Extended Data Fig.9a). Murine FHL1 interacts with CHIKV nsP3 and enhances viral infection, albeit less efficiently that its human orthologue (Extended Data Fig.9 b-d). Moreover, CHIKV infection was strongly impaired in the murine muscle cell C2C12 deleted for the *fhl1* gene (Extended Data

Fig.9 e-f). Susceptibility to CHIKV infection of young mice deficient or not for FHL1 was then tested. CHIKV actively replicated in tissues of WT littermates, as previously reported[20], but virtually no infectious particles were detected in tissues of FHL1-null mice (Fig. 4a). Moreover, necrotizing myositis with massive infiltrates and necrosis of the muscle fibers were observed in skeletal muscle of WT littermates, while FHL-null mouse muscle showed no detectable pathology (Fig. 4b). Immunolabelling with Ab against CHIKV E2 protein, FHL1 and vimentin in muscle revealed that in young WT mice, CHIKV mainly targets muscle fiber expressing FHL1, whereas muscle cells of FHL1-null mice show no label for CHIKV nor for FHL1 (Fig. 4c). These experiments demonstrate that *FHL1* knock out mice are resistant to CHIKV infection.

In summary, this study shows that FHL1 is a critical CHIKV host dependency factor for infection and pathogenesis. *In vivo*, FHL1 expression pattern, which accounts for the clinical presentation of EDMD, also reflects CHIKV tissue tropism for skeletal muscles and joints. This suggests that the hijacking of FHL1 by CHIKV during infection may, on top of allowing viral replication, lead to cellular dysfunctions contributing to muscular and joint pains that are the hallmark of chikungunya disease[1,2]. Mechanistically, FHL1 interacts with the HVD domain of nsP3 to enable viral RNA synthesis and viral replication complex formation. The alphavirus nsP3 HVD domain is an intrinsically disordered region that binds distinct sets of cellular proteins[23,26,30] such as the G3BP1 and G3PB2, two key components and markers of stress granules that are important for the replication of CHIKV and other alphaviruses[22,26]. G3BP1/2 nsP3 interactions are thought drive a common alphavirus-specific mechanism that is important for assembly of the replication complex and stabilization of viral G RNA[22,23,26]. FHL1 interacts with a nsP3 HVD region which is located away from G3BP1/2 binding sites. Therefore, FHL1 and G3BP proteins likely play distinct roles

during CHIKV replication. In contrast to G3BPs, FHL1 is selectively used by CHIKV, suggesting that it may accomplish a specific and essential function in CHIKV RNA amplification. Upon interaction with FHL1, CHIKV nsP3 HVD may adopt a unique conformation that is critical for the initiation of viral replication. Interestingly, intrinsically disordered domains (IDD) such as the nsP3 HVD have also been shown to induce liquid-liquid phase separations[31] and negative-stranded RNA viruses use proteins displaying IDDs to form liquid organelles for their replication[32]. Indeed, in CHIK-infected cells, nsP3 forms intracellular granules reminiscent of these virus–induced inclusions [33,34]. FHL1 may regulate the formation and/or the dynamic of such granules to create an optimal environment for efficient CHIKV RNA amplification. FHL1 contains four LIM domains arranged in tandem known to function as a modular protein binding interface regulating diverse cellular pathways[35]. FHL1 has been shown to scaffold MAPK components (Raf-1/MEK2/ERK2) to the stretch sensor Titin N2B to transmit MAPK signals that regulate muscle compliance and cardiac hypertrophy[36,37]. One may speculate that, during CHIKV infection, FHL1 may be hijacked from its physiological function in sarcomere extensibility and intracellular signaling to act as scaffolding protein promoting CHIKV RNA amplification.

In conclusion, this study provides major insights into the understanding of CHIKV interactions with its target host cell. Although other host-factors have been identified as required for CHIKV infection, none of them fully account for the specific joint and muscular pathology which is the hallmark of CHIKV and gave its name to its associated disease, chikungunya, which means “that which bends up” in Makonde, to describe the posture of patient with muscle and joint pain. The hijacking of FHL1 by nsP3 during CHIKV infection is unique and constitutes a critical clue that paves the way to fully decipher the pathogenesis of chikungunya disease. Targeting FHL1A–

265 nsP3 interactions now stands as an attractive therapeutic approach to combat CHIKV
266 pathogenesis.
267

METHODS

Cell culture. HAP1 cells (Horizon Discovery), which are derived from near-haploid chronic myeloid leukemia KBM7 cells, were cultured in IMDM supplemented with 10% FBS, 1% penicillin-streptomycin (P/S) and GlutaMAX (Thermo Fisher Scientific). 293FT (Thermo Fisher Scientific), HEK-293T (ATCC), Vero E6 (ATCC), HepG2 (kind gift of Olivier Schwartz, Institut Pasteur, Paris, France), primary myoblasts and primary fibroblasts were cultured in DMEM supplemented with 10% FBS, 1% penicillin-streptomycin, 1% GlutaMAX and 25 mM Hepes. Human placenta choriocarcinoma Bewo cells were cultured in in DMEM supplemented with 5% FBS, 1% penicillin-streptomycin, 1% GlutaMAX and 25 mM Hepes. AP61 mosquito (Aedes pseudoscutellaris) cells (gift from Philippe Despres, Institut Pasteur, Paris, France) were cultured at 28°C in Leibovitz medium supplemented with 10% FCS, 1% P/S, 1% glutamine, 1X non-essential amino acid, 1X Tryptose phosphate and 10 mM Hepes. All cell lines were cultured at 37°C in presence of 5% CO_2 with the exception of AP61 that were maintained at 28°C with no CO_2.

Virus strains and culture. CHIKV21 (strain 06-21), ZIKV (HD78788) (both are kind gift from Philippe Despres, Institut Pasteur, Paris, France), CHIKV West Africa (strain 37997, accession nb AY726732.1) and dengue virus serotype 2 DENV (16681) viruses were propagated in mosquito AP61 cell monolayers with limited cell passages. CHIKV-Brazza-MRS1 2011, CHIKV-Ross, CHIKV-St Martin H20235 2013-Asian, RRV (strain 528v), MAYV (strain TC 625), ONNV (strain Dakar 234), SINV (strain Egypt 339), EEEV (strain H178/99), VEEV (strain TV83 vaccine), WEEV (strain 47A), SFV (strain 1745) were obtained from the European Virus Archive (EVA) collection and propagated with limited passage on Vero E6 cells.

pCHIKV-M-Gluc (see plasmid sections) and pCHIKV-mCherry molecular clones were derivate of pCHIKV-M constructed from a CHIKV (strain BNI-CHIKV_899) isolated from a patient during Mauritius outbreak in 2006. To generate infectious virus from CHIKV molecular clones, capped viral RNAs were generated from the NotI-linearized CHIKV plasmids using a mMESSAGE mMACHINE SP6 or T7 Transcription Kit (Thermo Fischer Scientific) according to manufacturer's instructions. Resulting RNAs were purified by phenol:chloroform extraction and isopropanol precipitation, resuspended in water, aliquoted and stored at -80°C until use. Thirty µg of purified RNAs were transfected in BHK21 with lipofectamine 3000 reagent and supernatants harvested 72 hours later were used for viral propagation on Vero E6 cells.

For all the viral stock used in flow cytometry analysis experiments, viruses were purified through a 20% sucrose cushion by ultracentrifugation at 80,000xg for 2 hours at 4°C. Pellets were resuspended in HNE1X pH7.4 (Hepes 5 mM, NaCl 150 mM, EDTA 0.1 mM), aliquoted and stored at -80°C. Viral stock titers were determined on Vero E6 cell by plaque assay and are expressed as PFU per ml. Virus stocks were also determined by flow cytometry as previously described [38,39] Briefly, Vero E6 cells were incubated for 1h with 100µl of 10-fold serial dilutions of viral stocks. The inoculum was then replaced with 500µl of culture medium and the percent of E2 expressing cells was quantified by flow cytometry at 8 hpi. Virus titers were calculated using the following formula and expressed as FACS Infectious Units (FIU) per ml. [Titer (FIU/ml) = (average % of infection) x (number of cells in well) x (dilution factor) / (ml of inoculum added to cells)].

Reagents. . The following antibodies were used: anti-FHL1 mAb (ref MAB5938, R & D Systems), anti-FHL1 rabbit Ab (ref NBP1-88745, Novus Biologicals), anti-vimentin

antibody (ab24525, abcam), anti-GAPDH mAb (ref SC-47724, Santa Cruz Biotechnology), polyclonal rabbit anti-HA (ref 3724, Cell Signaling Technology), anti-FLAG M2 mAb (ref F1804, SIGMA), anti-RFP (ref 6G6, Chromotek), anti-CHIKV E2 mAb (3E4 and 3E4 conjugated-CY3), anti-alphavirus E2 mAb (CHIK-265 was a kind gift from Michael Diamonds, University school of medicine, St Louis, USA), anti-EEEV E1 mAb (ref MAB8754, Sigma), anti-pan-flavivirus E protein mAb (4G2), anti-dsRNA J2 mAb (Scicons), Alexa Fluor™ 488-conjugated goat anti-rabbit IgG (A11034, Invitrogen), Alexa Fluor™-647-conjugated goat anti-chicken IgG (ab150175, abcam), Alexa Fluor™ 488-conjugated goat anti-mouse IgG (115-545-003, Jackson ImmunoResearch), Alexa Fluor™ 647-conjugated goat anti-mouse IgG (115-606-062, Jackson ImmunoResearch), peroxydase-conjugated donkey anti-rabbit IgG (711-035-152, Jackson ImmunoResearch), and anti-mouse/HRP (P0260, Dako Cytomotion). FLAG magnetic beads (ref M8823, SIGMA), HA-magnetic beads (ref 88837, Thermo Fisher Scientific) and anti-RFP coupled to magnetic agarose beads (RFP-Trap MA, Chromotek) were used for immunoprecipitation experiments.

CRISPR genetic screen. The GeCKO v2 human CRISPR pooled libraries (A and B) encompassing 123,411 different sgRNA targeting 19,050 genes (cloned in the plentiCRISPR v2) were purchased from GenScript. Lentiviral production was prepared independently for each half-library in 293FT cells by co-transfecting sgRNA plasmids with psPAX2 (Kind gift from Nicolas Manel, Institut Curie, Paris, France) and pCMV-VSV-G at a ratio of 4:3:1 with lipofectamine 3000 (Thermo Fisher Scientific). Supernatants were harvested 48h after transfection, cleared by centrifugation (750 x g for 10 min), filtered using a 0.45 µM filter and purified through a 20% sucrose cushion by ultracentrifugation (80,000 x g for 2 hours at 4°C). Pellets were resuspended in

HNE1X pH7.4, aliquoted and stored at -80°C. HAP1 cells were transduced by spinoculation (750 x g for 2 hours at 32°C) with each CRISPR-sgRNA lentiviral libraries at a multiplicity of infection (MOI) of 0.3 and a coverage of 500 times the sgRNA representation. Cells were selected with puromycin for 8 days and expanded. Sixty million cells from each library were pooled and infected with CHIKV21 using a MOI of 1. Simultaneously forty million of non-infected pooled cells were pelleted and kept at -80°C to serve as a reference of the library representation at time of infection. Approximately 5 days after infection, cytopathic effect was detectable and surviving cells were collected 2 weeks later. Genomic DNA was extracted from selected cells or non-infected pooled cells using QIAamp DNA column (Qiagen), and inserted gRNA sequences were amplified and subject to next generation sequencing on an Illumina MiSeq (Plateforme MGX, Institut Génomique Fonctionelle, Montpellier, France). gRNA sequences were analyzed using the MAGeCK software [13]. Additionaly, gRNA sequences were analyzed using the RIGER software following previously published recommendation[40].

FHL1 editing. FHL1 was validated using two independent sgRNA targeting the exon 3 and exon 4, which are common to all FHL1 isoforms. sgRNA1, 5'-GAGGACTCCCCCAAGTGCAA-3' and sgRNA2, 5'-GCAGTCAAACTTCTCCGCCA-3' were cloned into the plasmid lentiCRISPR v2 according to Zhang lab's recommendation. HAP1 and 293FT cells were transiently transfected with the plasmid expressing individual sgRNA and selected with puromycin until all mock-transfected cells died (approximately 72 hours). Transfected cells were used to ascertain gRNA-driven resistance to CHIKV cytopathic effect, and clonal cell lines were isolated by limiting dilution and assessed by immunoblot for FHL1 expression.

Infection assay. For infection quantification by flow cytometry analysis, cells were plated in 24-well plates. Cells were infected for 24 (293T) or 48 hours (HAP1), trypsinized and fixed with 2% (v/v) paraformaldehyde (PFA) diluted in PBS for 15 min at room temperature. Cells were incubated for 30 min at 4°C with 1µg/ml of either the 3E4 anti-E2 mAb for CHIKV strains and ONNV) or the CHIKV 265 anti-E2 mAb for MAYV or the anti-E1 mAb for EEEV or anti-pan-flavivirus E 4G2 for DENV and ZIKV. Ab were diluted in permeabilization flow cytometry buffer (PBS supplemented with 5% FBS, 0.5% (w/v) saponin, 0.1% Sodium azide). After washing, cells were incubated with 1µg/ml of Alexa Fluor 488 or 647-conjugated goat anti-mouse IgG diluted in permeabilization flow cytometry buffer for 30 min at 4°C. Acquisition was performed on an Attune NxT Flow Cytometer (Thermo Fisher Scientific) and analysis was done by using FlowJo software (Tree Star). To assess infectious viral particles release during infection, cells were inoculated for 3 hours with viruses, washed once and then maintained in culture medium over a 72-hour period. At indicated time points supernatants were collected and kept at -80°C. Vero E6 cells were incubated with 10-fold serial dilution of supernatant for 24 hours and E2 expression was quantified by flow cytometry as described above.

For detection of infected cells by immunofluorescence, control and ΔFHL1 HAP1 cells were plated on Lab-Tek II CC2 glass slide 8 wells (Nunc). Cells were inoculated with CHIKV21 strain (MOI of 20) or CHIKV-nsP3-mCherry (MOI of 20) for 48 hours, then washed thrice with cold PBS and fixed with 4% (v/v) PFA diluted in PBS for 20 min at room temperature. CHIKV E2 protein was stained with the 3E4 mAb at 5 µg/ml, followed by a secondary staining with 1µg/ml of Alexa 488-conjugated goat anti-mouse IgG. Both antibodies were diluted in PBS supplemented with 3% (w/v) BSA and 0.1%

saponin. Slides were mounted with ProLong Gold antifade reagent containing 4,6-diamidino-2-phenylindole (DAPI) for nuclei staining (Thermo Fisher Scientific).

For colocalization experiments, cells infected with CHIKV-nsP3-mCherry (MOI of 20) were stained with 10 µg/ml of the anti-FHL1 mAb, followed by a secondary staining with 1µg/ml of Alexa 488-conjugated goat anti-mouse IgG.

For detection of dsRNA foci, control and ΔFHL1 293T cells were plated on Lab-Tek II CC2 glass slide 8 wells (Nunc) and infected with CHIKV21 strain (MOI of 50) for 4 or 6 hours. After fixation with 4% (v/v) PFA diluted in PBS, cells were stained with 5 µg/ml of the anti-dsRNA mAb, followed by a secondary staining with 1µg/ml of Alexa 488-conjugated goat anti-mouse IgG. Both antibodies were diluted in PBS supplemented with 3% (w/v) BSA and 0.1% Triton 100X. Of note, no dsRNA foci were detectable at 4hpi.

Fluorescence microscopy images were acquired using a LSM 800 confocal microscope (Zeiss).

Plasmid constructions. To generate the C-terminal HA-tagged FHL1 isoforms, the cDNAs of FHL1A (NM_001449.4), FHL1B (XM_006724746.2) and FHL1C (NM_001159703.1) were purchased from Genscript. Coding sequence (CDS) were amplified with a common FHL1 Fwd primer 5'-CCGGA**GAATTC**GCCGCCATGGCGGAGAAGTTTGACTGCCACTACTGC-3'; and specific FHL1A Rev primer 5'-AATAGTTTA**GCGGCCGC**TCAAGCGTAATCTGGAA CATCGTATGGGTATCCTCCAGCGGCCGACAGCTTTTTGGCACAGTCGGGACAA TACACTTGCTCC-3'; or FHL1B and C specific Rev primer 5'-AATAGTTTA**GCGGCCGC**TCAAGCGTAATCTGGAACATCGTATGGGTATCCTCCA GCGGCCGACGGAGCATTTTTTGCAGTGGAAGCAGTAGTCGTGCC-3' (underline,

segment hybridizing with the target sequence; bold, restriction endonuclease site for cloning); and cloned into pLVX-IRES-ZsGreen1 vector (Takara). Using the same approach, coding sequence of murine FHL1 (NM_001077362.2) was amplified with a mFHL1 Fwd primer 5'-CCGGAGAATTCGCCGCCATGGCTTCTCAAAGACACTCAG GTCCCTCC-3' and mFHL1 Rev primer 5'-AATAGTTTAGCGGCCGCTCAAGCGTAA TCTGGAACATCGTATGGGTATCCTCCAGCGGCCGACAGCTTTTTGGCACAGTCA GGGCAATACACCGCTC-3', and cloned into pLVX-IRES-ZsGreen1 vector. C-terminal HA-tagged FHL2 coding sequence was synthesized by Genscript and subcloned into pLVX-IRES-ZsGreen1 vector. The plasmids pCI-neo-3×FLAG plasmids expressing the CHIKV nsP3 and nsP4, the Sindbis virus (SINV) and Semliki Forest virus (SFV) nsP3 proteins were previously described[41]. The CHIKV nsP3 ΔHVD, ΔR1 to ΔR4 were generated by site-directed mutagenesis (QuickChange XL Site-Directed Mutagenesis Kit, Agilent) using the following sets of primers: ΔHVD-Fwd (5'-CGTAAGTCCAAGGGAATATTGATGATCTTCCCAGGAGTCTGC-3') and ΔHVD-Rev (5'-GCAGACTCCTGGGAAGATCATCAATATTCCCTTGGACTTACG-3'); ΔR1-F: (5'-GTACCTGTCGCGCCGCCCAGAGAGCTGTGTCCGGTCGTACAAGA AAC-3') and ΔR1-R: (5'-GTTTCTTGTACGACCGGACACAGCTCTCTGGGCGGCG CGACAGGTAC-3'); ΔR2-F: (5'-GAAACAGCGGAGACGCGTGACAGTACCGCCA CGGAACCGAATC-3') and ΔR2-R: (5'-GATTCGGTTCCGTGGCGGTACTGTCACGC GTCTCCGCTGTTTC-3'); ΔR3-F: (5'-CTTCTTACCAGGAGAAGTGTGATGACTTGA CAGACAGC-3') and ΔR3-R: (5'-GCTGTCTGTCAAGTCATCACACTTCTCCTGGTAA GAAG-3'); ΔR4-F (5'-GACGAGAGAGAAGGGAATATAACACCGAGTACCGCCACG GAACCGAATC-3') and ΔR4-R (5'-GATTCGGTTCCGTGGCGGTACTCGGTGTTATA TTCCCTTCTCTCTCGTC-3').

The plasmids expressing the chimeric nsP3 CHIKV-HVD SINV and nsP3 SINV-HVD CHIKV were obtained as follows. First, the DNA sequence coding for the N-terminal parts of the CHIKV or SINV nsP3 (MD-AUD region) are obtained by PCR using the pCI-neo-3×FLAG expression plasmids as templates and the following sets of primers: 3xFLAG_NotI-F (5'-ACTGAGCGGCCGCATGGACTACAAAGACCATGAC-3') and Overlap-CHIKV-SINV-R (5'-GCTGTTCTGGCACTTCTATATATTCCCTTGGA CTTACG-3'), or 3xFLAG_NotI-F and Overlap-SINV-CHIKV-R (5'-CAGACTCCTGGGAAGATCTGTACTTACGGGCGGGAAC-3') for CHIKV and SINV constructs, respectively. HVD coding sequences were also generated by PCR using the following primers: Overlap-CHIKV-SINV-F (5'-CGTAAGTCCAAGGGAATATATAGAAGTGCCAGAACAGC-3') and nsP3-SINV_BamHI-R (5'-ACTGAGGATCCTTAGTATTCAGTCCTCCTGCTC-3') for SINV HVD, and Overlap-SINV-CHIKV-F (5'-GTTCCCGCCCGTAAGTACAGATCTTCCCA GGAGTCTG-3') and nsP3-CHIKV_BamHI-R (5'-ACTGAGGATCCTCATAACTCGT CGTCCGTG-3') for CHIKV HVD. Next, the CHIKV-HVD-SINV and SINV-HVD-CHIKV PCR-fragments were obtained by overlap extension PCR using the previously obtained PCR-products and the following sets of primers: 3XFLAG_NotI-F and nsP3-SINV_BamHI-R or nsP3-CHIKV_BamHI-R. Finally, the chimeric PCR fragments were cloned into a NotI-BamHI digested pLVX-IRES-ZsGreen1 vector (Takara).

The plasmid expressing FHL1A-R4 and FHL1A-R4* fusion proteins were obtained by overlap extension PCR approach as well. First, the FHL1A part which is common to both constructs was amplified from a cDNA template (Genscript, NM_001449.4) using the common FHL1 Fwd primer (5'-CCGGAGAATTCGCCGCCATGGCGGAGAAGTTTGACTGCCACTACTGC-3') and the Overlap-FHL1A-Fusion Rev primer (5'- CGCCCTGGAAGTACAGGTTCTCGCCG

CCGCCCAGCTTTTTGGCACAGTCGGGACAATAC-3'). Second, nsP3-R4 and –R4* portions were obtained by PCR using either the pCI-neo-3×FLAG-nsP3 expression plasmid or the pCHIKV-SG45-R4* plasmid (containing the randomized R4 region) as templates and the following set of primers: Overlap-FHL1-fusion-Fwd (5'-CGAGAACCTGTACTTCCAGGGCGGCGGCGGCCCCATGGCTAGCGTCCGATTCTTTAG-3') and FHL1-fusion-Rev (5'-AATAGTTTAGCGGCCGCTCAAGCGTAATCTGGAACATCGTATGGGTAGCCGCCGCCCGGTGGTGCCTGAAGAGACATTGCTG-3') for R4 construct, or FHL1-fusion-Rand-Rev primer (5'-AATAGTTTAGCGGCCGCTCAAGCGTAATCTGGAACATCGTATGGGTAGCCGCCGCCCCTCACCTCGGCGCACATGG-3') for the randomized R4* construct. Next, the FHL1A-R4 and FHL1A-R4* PCR-fragments were obtained by PCR using the previously obtained PCR-products and the outer sets of primers: FHL1A Fwd and FHL1-fusion-Rev or FHL1-fusion-Rand-Rev. Amplification fragments were cloned into a NotI-EcoRI digested pLVX-IRES-ZsGreen1 vector (Takara).

To obtain pCHIKV-M-Gluc a viral sequence encompassing the CHIKV 26S promoter and a part of the capsid protein sequence was amplified from pCHIKV-M using primers 5'-TATGCGTTTAAACCATGGCCACCTTTGCAAGCTCCAGATC-3' and 5'-GCTTCTTATTCTTCCGATTCCTGCGTGG-3', cut with PmeI and BssHII and assembled together with an AgeI-PmeI fragment from pCHIKVRepl-Gluc[42] into an AgeI-BssHII cut vector. From the resulting plasmid the AgeI-BssHII fragment was released and ligated together with a BssHII-SfiI fragment from pCHIKV-M[43] into pCHIKV-M cut with AgeI and SfiI.

To establish pCHKV-Rluc-GAA two PCR fragments were amplified from pCHIKV-WT using primers CHIKV 5590 F (5'-AGACTTCTTACCAGGAGAAGTG-3') and Bo422 (5'-CGACTCCATGTATTATGTTacccgctgcGATGAAGGCCGCGCACGCGG-3') or Bo421

(5’-CCGCGTGCGCGGCCTTCATCgcagcgggtAACATAATACATGGAGTCG-3’) and CHIKV 8512 R (5’-GAAGTTGTCCTTGGTGCTGC-3’), respectively. The obtained fragments were fused via PCR amplification using the outer primers CHIKV 5590 F and CHIKV 8512 R. The resulting fragment was cut with AgeI and BglI and inserted into pCHIKV-Rluc cut with the same restriction enzymes.

For generation of CHIKV-Rluc-ΔR4 and CHIKV-Rluc-R4* first PCR fragments encompassing the desired changes were amplified and assembled as follows: 1) CHIKV-Rluc-ΔR4: two fragments amplified from CHIKV-Rluc using Bo408 (5’-CACCACGTGCTCCTGGTCAGTG-3’) and Bo1259 (5’-gattcggttccgtggcggtactcggtgttatattcccttctctctcgtca-3’) or Bo1258 (5’-tgacgagagagaagggaatataacaccgagtaccgccacggaaccgaatc-3’) and Bo409 (5’-GACTTCCTCCAGGGTGTTCACC-3’), respectively, were fused together using the outer primers Bo408 and Bo409. 2) CHIKV-Rluc-R4*: the randomized sequence cassette was obtained sequentially from three successive PCRs: First PCR fragment was generated using primers Bo1260 (5’-AGCACCGTGCCCCTGCCCGCCCTGAGGAGGGCCAGCTTCGCCGACACCATGG AGCAGACC-3’) and Bo1261 (5’-CCTCACCTCGGCGCACATGGGGAACTGCTCGGCCACGGTCTGCTCCATGGTGT CGGCGAA-3’). Then, it was fused at the 5’ end with a PCR fragment amplified from CHIKV-Rluc with Bo408 and Bo1262 (5’-TCAGGGCGGGCAGGGGCACGGTGCTtgttatattcccttctctctcgtca-3’). Next, the resulting fragment is further fused at the 3’ end with a PCR fragment amplified from CHIKV-Rluc with Bo1263 (5’-GTTCCCCATGTGCGCCGAGGTGAGGccgagtaccgccacggaaccgaatc-3’) and Bo409, using the outer primers Bo408 and Bo409. Finally, the PCR fragments containing the

517 ΔR4 and R4* mutations were cut with SacII and AgeI and fused in each case with a
518 NgoMIV-SacII fragment derived from CHIKV-Rluc (SG45) and were cloned into a
519 NgoMIV-AgeI digested SG45 plasmid.
520
521 **Trans-complementation and over expression experiments.** The lentiviral plasmids
522 containing FHL1 isoforms were packaged as described above (see 'CRISPR genetic
523 screen' section). Cells of interest were stably transduced by spinoculation (750 x g for
524 2 hours at 32°C) with these lentiviruses and, when necessary, sorted for GFP-positive
525 cells by flow cytometry. For trans-complementation assays cells were inoculated with
526 CHIKV21 for 48 hours. Cells were then collected and processed for E2 expression by
527 flow cytometry. For ectopic expression, cells were plated on 24-well plates ($5x10^4$) and
528 incubated with CHIKV-M-GLuc and CHIKV21, and either processed for E2 expression
529 by flow cytometry or infectious virus yield quantification on Vero E6 cells.
530
531 **Kinetic of infection by qPCR assay.** Control and ΔFHL1 HAP1 cells were plated on
532 60 mm dishes (400,000 cells) and inoculated with CHIKV21 (MOI of 5). At indicated
533 time point cells were washed thrice with PBS, incubated with trypsin 0.25% for 5 min
534 at 37°C to remove cells surface bound particles, and total RNA was extracted using
535 the RNeasy plus mini kit (Qiagen) according to manufacturer's instruction. cDNAs were
536 generated from 500 ng total RNA by using the Maxima First Strand Synthesis Kit
537 following manufacturer's instruction (Thermo Fisher Scientific). Amplification products
538 were incubated with 1 Unit of RNAse H for 20 min at 37 °C, followed by 10 min at 72°C
539 for enzyme inactivation, and diluted 10-fold in DNAse/RNAse free water. Real time
540 quantitative PCR was performed using a Power Syber green PCR master Mix (Fisher
541 Thermo Scientific) on a Light Cycler 480 (Roche). The primers used for qPCR were:

E1-C21_F (5'-ACGCAGTTGAGCGAAGCAC-3'), E1-C21_R (5'-CTGAAGACATTG GCCCCAC-3') for viral RNA quantification, and Quantitect primers for GAPDH were purchased from Qiagen. The relative expression quantification was performed based on the comparative threshold cycle (C_T) method, using GAPDH as endogenous reference control. CHIKV negative strand RNA was quantified as previously described[44] . Briefly, cDNA were generated from 1µg total RNA using a primer containing a 5' tag sequence CHIKV(-)Tag (5'-GGCAGTATCGTGAATTCGATGCCGCTGTACCGTCCCCATTCC-3') and the SuperScript II reverse transcriptase following the manufacturer's instruction (Thermo Fisher Scientific). Amplifications products were diluted 10-fold and used for real time quantitative PCR with the following primers CHIKV(-)fwd (5'-GGCAGTATCGTGAATTCGATGC-3') and CHIKV(-)rev (5'-ACTGCTGAGTCCAAAG TGGG-3'). The 133 bp sequence corresponding to the amplified cDNA was synthesized by Genescript and serially diluted (650 to $6.5x10^9$ genes copies/µl) to generate standard curves.

Genomic viral RNA transfection and kinetic of viral amplification. To assess CHIKV RNA replication within the cells, we transfected control and ΔFHL1 cells with capped genomic viral RNA generated from pCHIKV-M-Gluc (see 'Virus strains and culture' section). Cells were plated on 48 well plate ($3x10^4$ cells) and transfected with 100 ng of purified RNA using the Lipofectamine MessengerMax reagent according to the manufacturer's instruction (Thermo Fisher Science), and cells were cultured in absence or presence of 15 mM NH_4Cl to prevent subsequent viral propagation. At specific times, cells were washed once with PBS and lyzed with Gaussia lysis buffer. Lysates were kept at -20°C until all samples were collected. Luciferase activity was

567 measured by using the Pierce Gaussia Luciferase Glow assay kit on a TriStar2 LB 942
568 with 20 µl of cell lysate, 20 µl of substrate and 2s integration time.
569 The same experimental approach was used to monitor luciferase activity from capped
570 genomic viral RNA generated from pCHIKV-Rluc WT (SG45), pCHIKV-Rluc-GAA,
571 pCHIKV-Rluc-ΔR4 and pCHIKV-Rluc-R4* mutants. Luciferase activity was measured
572 using the Renilla Luciferase assay system (Promega) on a TriStar2 LB 942 with 20 µl
573 of cell lysate, 20 µl of substrate and 2.5s integration time.
574
575 **Immunoblot.** Cell pellet were lysed in Pierce™ IP Lysis Buffer (Thermo Fisher
576 Scientific) containing Halt™ Protease and Phosphatase Inhibitor Cocktail (Thermo
577 Fischer Scientific) for 30 min at 4°C. Equal amount of protein, determined by
578 DC™Protein Assay (BioRad), were prepared in LDS Sample Buffer 4X (Pierce™)
579 containing 25 mM dithiothreitol (DTT) and heated at 95°C for 5 min. Samples were
580 separated on Bolt™ 4-12% Bis-Tris gels in Bolt® MOPS SDS Running Buffer (Thermo
581 Scientific), and proteins were transferred onto a PVDF membrane (BioRad) using the
582 Power Blotter system (Thermo Fischer Scientific). Membranes were blocked with PBS
583 containing 0.1% Tween-20 and 5% non-fat dry milk and incubated overnight at 4°C
584 with primary antibody. Staining was revealed with corresponding horseradish
585 peroxidase (HRP)-coupled secondary antibodies and developed using SuperSignal™
586 West Dura Extended Duration Substrate (Thermo Fisher Scientific) following
587 manufacturer's instructions. The signals were acquired through Fusion Fx camera
588 (VILBERT Lourmat).
589
590 **Co-immunoprecipitation assay.** HEK-293T cells were plated in 10 cm dishes (5.10^6
591 cells/ dish). Twenty-four hours later, the cells were transfected with a total of 15 µg of

DNA expression plasmids (7.5 µg of each plasmid in co-transfection assays). Twenty-four hours post-transfection the cells washed once with PBS and collected with a cell scrapper. After 5 min centrifugation (400 x g for 5 min), cells pellets were lysed for 30 min in cold IP lysis buffer supplemented with Halt™ Protease and Phosphatase Inhibitor Cocktail, and then cleared by centrifugation for 15 min at 6,000 x g. Supernatants were incubated overnight at 4°C, with either anti-FLAG magnetic beads or HA magnetic beads (see 'reagent' section above). Beads were washed three times with BO15 buffer (20 mM Tris-HCl pH 7.4, 150 mM NaCl, 5 mM MgCl2, 10% Glycerol, 0.5 mM EDTA, 0.05% Triton, 0.1% Tween-20). The retained complexes were eluted twice with either 3xFLAG-peptide (200 µg/ml; SIGMA F4799-4MG) or HA peptide (400 µg/ml; Roche# 11666975001) for 30 min at room temperature. Samples were prepared and subjected to immunoblot as described above. For input, 1% of whole cell lysate were loaded on the gel.

Bacterial expression, purification and GST pull down assay. To express nsP3, nsP3ΔHVD as glutathione S-transferase fusion proteins, their respective open reading frame (orf) were subcloned into pGEX-4T-1. Similarly, FHL1A cDNA was subcloned into the pET47b (+) and expressed as a 6xHis fusion protein. The following oligonucleotides were used to amplify nsP3 and nsP3ΔHVD cDNAs (sense: 5'-ccccggaattcATGgcaccgtcgtaccgggtaa-3'; antisense: 5'-ccgctcgagTCAtaactcgtcgtccgtgtctg-3') and FHL1A (sense: 5'-ccggaattccATGgcggagaagtttgactgcc-3'; antisense: 5'-ccgctcgagTTAcagctttttggcacagtc-3'). E.Coli strain BL21 Star (Invitrogen) was transformed with recombinant expression vectors encoding GST-nsP3, GST-nsP3ΔHVD or 6xHis-FHL1A recombinant proteins. Transformed bacteria were

induced with isopropylthio-β-Dgalactoside (IPTG) for 3 hours at 37°C. Cells were collected by centrifugation and the pellets were resuspended in lysis buffer containing lysozyme (1 mg/mL), incubated 30 min at 4°C followed by three subsequent freeze-thawed cycles and sonication. The bacterial lysates were centrifuged at 13,000 r.p.m for 20 min and the supernatants were incubated with glutathione-Sepharose beads for GST-nsP3 and GST-nsP3ΔHVD, or Ni-NTA column (Qiagen) for 6xHis-FHL1A. Column washing and recombinant protein elution were performed according to the manufacturer's instructions. Five µL of eluted GST fusion proteins and 3 µL of Ni-NTA eluted 6xHis-FHL1A were analyzed by SDS-PAGE and proteins were visualized by Coomassie staining. For pull-down assay, GST, GST-nsP3 or GST-nsP3ΔHVD bound beads were incubated with 6xHis-FHL1A for 1 hour at 4°C in presence of 100 µM $ZnSO_4$. The resin was washed extensively with a buffer containing 500 mM KCL. The beads were then resuspended in Laemmli buffer, resolved on SDS-PAGE and the presence of 6xHis-FHL1A was assessed by western blot using anti-FHL1 antibody.

Genetic analysis, fibroblasts and myoblasts from Emery-Dreifuss muscular dystrophy patients. Dermal fibroblasts and myoblasts were taken from 4 patients carrying *FHL1* gene mutations. *FHL1* gene was analyzed as previously reported [6] as they had, among other symptoms, features reminiscent of Emery-Dreifuss muscular dystrophy. Patients P1, P2 and P3 were previously reported [6] with detailed clinical description (respectively as patient F321-3, F997-8 and F1328-4) while patient P4 was not yet published. Briefly, patient P4 had myopathy with joint contractures, hypertrophic cardiomyopathy, vocal cords palsy, short stature, alopecia, skin abnormalities and facial dysmorphism. In this patient, *FHL1* analysis revealed an insertion of a full-length LINE-1 retrotransposon sequence together with poly A tail of unknown length (i.e.,?

642 thereafter) after 27 bp of the start of exon 4 (c.183_184ins [LINE1;?; 171_183]) that
643 results at mRNA level in altered splicing with retention of 108 bp of the inserted LINE
644 sequence leading to predicted premature termination codon and shorter FHL1A
645 (Extended Data Fig. 7b).
646
647 **Ethics statement.** All materials (skin and/or muscle biopsies) from patients and
648 controls included in this study were taken with the informed consent of the donors and
649 with approval of the local ethical boards. All the procedures were followed alongside
650 the usual molecular diagnostic procedure during patient follow-up, and in accordance
651 with the ethical standards of the responsible national committee on human
652 experimentation.
653
654 **In vivo studies.** Animals were housed in the Institut Pasteur animal facilities
655 accredited by the French Ministry of Agriculture for performing experiments on live
656 rodents. Work on animals was performed in compliance with French and European
657 regulations on care and protection of laboratory animals (EC Directive 2010/63, French
658 Law 2013-118, February 6th, 2013). All experiments were approved by the Ethics
659 Committee #89 (and registered under the reference APAFIS#6954-
660 2016091410257906 v2). Male mice either deficient for FHL1 (FHL1-null) or not (WT
661 littermates) were obtained by crossing heterozygous females for FHL1[45] with WT male
662 Black Swiss mice. Nine day-old male littermates, both FHL1-null and WT mice, were
663 injected with CHIKV21 (10^5 PFU/20µl) by intradermal route and viral load was
664 determined in tissues by day 7 post infection. Virus titers in tissue samples were
665 determined on Vero E6 cells by tissue cytopathic infectious dose 50 (TCID50/g). For
666 histology experiments, muscles were snap frozen in isopentane cooled by liquid

nitrogen for cryo-sectioning then processed for histological staining (hematoxylin and eosin) or immunolabelling.

Transmission electron microscopy. Cells were scrapped and fixed for 24 h in 1% glutaraldehyde, 4% paraformaldehyde, (Sigma, St-Louis, MO) in 0.1 M phosphate buffer (pH 7.2). Samples were then washed in phosphate-buffered saline (PBS) and post-fixed for 1 h by incubation with 2% osmium tetroxide (Agar Scientific, Stansted, UK). Cells were then fully dehydrated in a graded series of ethanol solutions and propylene oxide. Impregnation step was performed with a mixture of (1∶1) propylene oxide/Epon resin (Sigma) and then left overnight in pure resin. Samples were then embedded in Epon resin (Sigma), which was allowed to polymerize for 48 hours at 60°C. Ultra-thin sections (90 nm) of these blocks were obtained with a Leica EM UC7 ultramicrotome (Wetzlar, Germany). Sections were stained with 2% uranyl acetate (Agar Scientific), 5% lead citrate (Sigma) and observations were made with a transmission electron microscope (JEOL 1011, Tokyo, Japan).

Cell viability assay. Cell viability and proliferation were assessed using the CellTiter-Glo 2.0 Assay (Promega) according to the manufacturer's protocol. In brief, cells were plated in 48-well plates ($3x10^4$). At specific times, 100 µl of CellTiter-Glo reagent were added to each well. After 10 min incubation, 200 µl from each well were transferred to an opaque 96-well plate (Cellstar, Greiner bio-one) and luminescence was measured on a TriStar2 LB 942 (Berthold) with 0.1 second integration time.

Statistical analysis. Graphical representation and statistical analyses were performed using Prism7 software (GraphPad Software). Unless otherwise stated, results are

shown as means +/- standard deviation (SD) from at least 2 independent experiments in duplicates. Differences were tested for statistical significance using the unpaired two-tailed *t* test, One-way or Two-way Anova with multiple comparison post-test.

REFERENCES

1. Burt, F. J. *et al.* Chikungunya virus: an update on the biology and pathogenesis of this emerging pathogen. *Lancet Infect. Dis.* **17**, e107–e117 (2017).
2. Silva, L. A. & Dermody, T. S. Chikungunya virus: epidemiology, replication, disease mechanisms, and prospective intervention strategies. *J. Clin. Invest.* **127**, 737–749 (2017).
3. Weaver, S. C., Charlier, C., Vasilakis, N. & Lecuit, M. Zika, Chikungunya, and Other Emerging Vector-Borne Viral Diseases. *Annu. Rev. Med.* **69**, 395–408 (2018).
4. Greene, W. K., Baker, E., Rabbitts, T. H. & Kees, U. R. Genomic structure, tissue expression and chromosomal location of the LIM-only gene, SLIM1. *Gene* **232**, 203–207 (1999).
5. Schessl, J., Feldkirchner, S., Kubny, C. & Schoser, B. Reducing body myopathy and other FHL1-related muscular disorders. *Semin. Pediatr. Neurol.* **18**, 257–263 (2011).
6. Gueneau, L. *et al.* Mutations of the FHL1 gene cause Emery-Dreifuss muscular dystrophy. *Am. J. Hum. Genet.* **85**, 338–353 (2009).
7. Ooi, Y. S., Stiles, K. M., Liu, C. Y., Taylor, G. M. & Kielian, M. Genome-wide RNAi screen identifies novel host proteins required for alphavirus entry. *PLoS Pathog.* **9**, e1003835 (2013).
8. Karlas, A. *et al.* A human genome-wide loss-of-function screen identifies effective chikungunya antiviral drugs. *Nat. Commun.* **7**, 11320 (2016).
9. Zhang, R. *et al.* Mxra8 is a receptor for multiple arthritogenic alphaviruses. *Nature* **557**, 570–574 (2018).
10. Tanaka, A. *et al.* Genome-Wide Screening Uncovers the Significance of N-Sulfation of Heparan Sulfate as a Host Cell Factor for Chikungunya Virus Infection. *J. Virol.* **91**, 1_22 (2017).
11. Shalem, O. *et al.* Genome-scale CRISPR-Cas9 knockout screening in human cells. *Science* **343**, 84–87 (2014).
12. Schuffenecker, I. *et al.* Genome microevolution of chikungunya viruses causing the Indian Ocean outbreak. *PLoS Med.* **3**, e263 (2006).
13. Li, W. *et al.* MAGeCK enables robust identification of essential genes from genome-scale CRISPR/Cas9 knockout screens. *Genome Biol.* **15**, 554 (2014).
14. Shathasivam, T., Kislinger, T. & Gramolini, A. O. Genes, proteins and complexes: the multifaceted nature of FHL family proteins in diverse tissues. *J. Cell. Mol. Med.* **14**, 2702–2720 (2010).
15. Brown, S. *et al.* Characterization of two isoforms of the skeletal muscle LIM protein 1, SLIM1. Localization of SLIM1 at focal adhesions and the isoform slimmer in the nucleus of myoblasts and cytoplasm of myotubes suggests distinct roles in the cytoskeleton and in nuclear-cytoplasmic communication. *J. Biol. Chem.* **274**, 27083–27091 (1999).
16. Krempler, A., Kollers, S., Fries, R. & Brenig, B. Isolation and characterization of a new FHL1 variant (FHL1C) from porcine skeletal muscle. *Cytogenet. Cell Genet.* **90**, 106–114 (2000).
17. Pen, A. E. *et al.* A novel single nucleotide splice site mutation in FHL1 confirms an Emery-Dreifuss plus phenotype with pulmonary artery hypoplasia and facial dysmorphology. *Eur. J. Med. Genet.* **58**, 222–229 (2015).
18. Chan, K. K. *et al.* Molecular cloning and characterization of FHL2, a novel LIM domain protein preferentially expressed in human heart. *Gene* **210**, 345–350 (1998).
19. Rezza, G., Chen, R. & Weaver, S. C. O'nyong-nyong fever: a neglected mosquito-borne viral disease. *Pathog. Glob. Health* **111**, 271–275 (2017).
20. Couderc, T. *et al.* A mouse model for Chikungunya: young age and inefficient type-I interferon signaling are risk factors for severe disease. *PLoS Pathog.* **4**, e29 (2008).

745 21. Roberts, G. C. *et al.* Evaluation of a range of mammalian and mosquito cell lines for
746 use in Chikungunya virus research. *Sci. Rep.* **7**, 14641 (2017).
747 22. Scholte, F. E. M. *et al.* Stress granule components G3BP1 and G3BP2 play a proviral
748 role early in Chikungunya virus replication. *J. Virol.* **89**, 4457–4469 (2015).
749 23. Kim, D. Y. *et al.* New World and Old World Alphaviruses Have Evolved to Exploit
750 Different Components of Stress Granules, FXR and G3BP Proteins, for Assembly of Viral
751 Replication Complexes. *PLoS Pathog.* **12**, e1005810 (2016).
752 24. Jose, J., Taylor, A. B. & Kuhn, R. J. Spatial and Temporal Analysis of Alphavirus
753 Replication and Assembly in Mammalian and Mosquito Cells. *mBio* **8**, 1–16 (2017).
754 25. Götte, B., Liu, L. & McInerney, G. M. The Enigmatic Alphavirus Non-Structural
755 Protein 3 (nsP3) Revealing Its Secrets at Last. *Viruses* **10**, 1–26 (2018).
756 26. Meshram, C. D. *et al.* Multiple Host Factors Interact with Hypervariable Domain of
757 Chikungunya Virus nsP3 and Determine Viral Replication in Cell-Specific Mode. *J. Virol.*
758 (2018). doi:10.1128/JVI.00838-18
759 27. Mutso, M. *et al.* Mutation of CD2AP and SH3KBP1 Binding Motif in Alphavirus
760 nsP3 Hypervariable Domain Results in Attenuated Virus. *Viruses* **10**, (2018).
761 28. Schessl, J. *et al.* Proteomic identification of FHL1 as the protein mutated in human
762 reducing body myopathy. *J. Clin. Invest.* **118**, 904–912 (2008).
763 29. Bonne, G., Leturcq, F. & Ben Yaou, R. Emery-Dreifuss Muscular Dystrophy. in
764 *GeneReviews®* (eds. Adam, M. P. et al.) (University of Washington, Seattle, 1993).
765 30. Frolov, I., Kim, D. Y., Akhrymuk, M., Mobley, J. A. & Frolova, E. I. Hypervariable
766 Domain of Eastern Equine Encephalitis Virus nsP3 Redundantly Utilizes Multiple Cellular
767 Proteins for Replication Complex Assembly. *J. Virol.* **91**, (2017).
768 31. Uversky, V. N. Intrinsically disordered proteins in overcrowded milieu: Membrane-
769 less organelles, phase separation, and intrinsic disorder. *Curr. Opin. Struct. Biol.* **44**, 18–30
770 (2017).
771 32. Nikolic, J. *et al.* Negri bodies are viral factories with properties of liquid organelles.
772 *Nat. Commun.* **8**, 58 (2017).
773 33. Fros, J. J. *et al.* Chikungunya Virus nsP3 Blocks Stress Granule Assembly by
774 Recruitment of G3BP into Cytoplasmic Foci. *J. Virol.* **86**, 10873–10879 (2012).
775 34. Remenyi, R. *et al.* Persistent Replication of a Chikungunya Virus Replicon in Human
776 Cells Is Associated with Presence of Stable Cytoplasmic Granules Containing Nonstructural
777 Protein 3. *J. Virol.* **92**, (2018).
778 35. Kadrmas, J. L. & Beckerle, M. C. The LIM domain: from the cytoskeleton to the
779 nucleus. *Nat. Rev. Mol. Cell Biol.* **5**, 920–931 (2004).
780 36. Sheikh, F. *et al.* An FHL1-containing complex within the cardiomyocyte sarcomere
781 mediates hypertrophic biomechanical stress responses in mice. *J. Clin. Invest.* **118**, 3870–
782 3880 (2008).
783 37. Raskin, A. *et al.* A novel mechanism involving four-and-a-half LIM domain protein-1
784 and extracellular signal-regulated kinase-2 regulates titin phosphorylation and mechanics. *J.
785 Biol. Chem.* **287**, 29273–29284 (2012).
786 38. Medina, F. *et al.* Dengue virus: isolation, propagation, quantification, and storage.
787 *Curr. Protoc. Microbiol.* **Chapter 15**, Unit 15D.2. (2012).
788 39. Meertens, L. *et al.* The TIM and TAM families of phosphatidylserine receptors
789 mediate dengue virus entry. *Cell Host Microbe* **12**, 544–557 (2012).
790 40. Joung, J. *et al.* Genome-scale CRISPR-Cas9 knockout and transcriptional activation
791 screening. *Nat. Protoc.* **12**, 828–863 (2017).
792 41. Pellet, J. *et al.* ViralORFeome: an integrated database to generate a versatile collection
793 of viral ORFs. *Nucleic Acids Res.* **38**, D371-378 (2010).
794 42. Gläsker, S. *et al.* Virus replicon particle based Chikungunya virus neutralization assay

using Gaussia luciferase as readout. *Virol. J.* **10**, 235 (2013).
43. Kümmerer, B. M., Grywna, K., Gläsker, S., Wieseler, J. & Drosten, C. Construction of an infectious Chikungunya virus cDNA clone and stable insertion of mCherry reporter genes at two different sites. *J. Gen. Virol.* **93**, 1991–1995 (2012).
44. Plaskon, N. E., Adelman, Z. N. & Myles, K. M. Accurate strand-specific quantification of viral RNA. *PloS One* **4**, e7468 (2009).
45. Domenighetti, A. A. *et al.* Loss of FHL1 induces an age-dependent skeletal muscle myopathy associated with myofibrillar and intermyofibrillar disorganization in mice. *Hum. Mol. Genet.* **23**, 209–225 (2014).

ACKNOWLEDGMENTS

This study has received funding from the French Government's Investissement d'Avenir program, Laboratoire d'Excellence "Integrative Biology of Emerging Infectious Diseases" (grant n°ANR-10-LABX-62-IBEID), the “Investissements d’Avenir” program ANR-10-IHUB-0002, the ANR-15-CE15-00029 ZIKAHOST, Institut Pasteur, Inserm and European Research Council. Viruses were graciously provided by the Europe and Virus Archive, which has received funding from the European Union's Horizon 2020 research and innovation program under grant agreement No 653316. The authors thank Félix Rey, Olivier Schwartz, Nicolas Manel, Yves Gaudin, Jan Hellert, Marie-Laure Chaix, Stéphane Marot, Sylvain Chawki, Antoine Canat, Alessia Zamborlini, and Hugues de Thé for critical readings of the manuscript and helpful discussions. The authors thank Pierre Thouvenot and David Hardy for technical assistance and Ju Chen and Julius Bogomolovas from UC San Diego (CA, USA) for providing FHL1 knockout mice. The authors are grateful to Mike Diamond and Julie Fox (Washington University School of Medecine, Saint Louis, MO, USA) and Frederic Tangy (Institut Pasteur, France) for providing us with the anti-CHIKV 265 mAb and the alphavirus nsP1-4 constructs, respectively.

AUTHORS’ CONTRIBUTIONS

L.M. and A.A. conceived the study. L.M, M.L.H, T.C, V.K, A.B, L.B.M, C.D., M.L and A.A designed the experiments. L.M. performed the CRISPR-Cas9 screening and infection studies with L.B.M. M.L.H characterized the FHL1 and nsP3 interactions and performed the immunoprecipitation and western blot studies with the help of V.K. A.L. validated the FHL1 gRNA and generated the FHL1 knockout cells described in this study. A.B. performed the immunofluorescence microscopy experiments and infection

studies. L.M. and E.S.L. analyzed the gRNA sequencing and identified the hits. J.B.G and P.R. performed the EM experiments. C.D. and M.B performed the GST-pull experiments. B.M.K generated the CHIKV molecular clones described in this study and P.O.V provided key CHIKV reagents. L.P and X.L. provided the alphavirus strains and performed infection studies. T.C. and M.L. performed in vivo studies and provided expertise in the design of CHIKV experiments. S.R. performed virus titration assays and mice genotyping. T.G. performed immunofluorescence experiments in mice tissues with T.C. A.T.B, R.B.Y., L.G., R.J.M. and G.B provided myoblasts and fibroblasts from EDMD patients and the description of a new *FHL1* mutation in EDMD disease. L.M and AA wrote the initial manuscript draft, and the other authors contributed to editing into its final form.

FIGURE LEGENDS

Figure 1. **FHL1 is important for infection by CHIKV and ONNV**

a, Results of the CHIKV screen analyzed by MAGeCK. Each circle represents individual gene. Y-axis represents the significance of sgRNA enrichment of genes in the selected population compared to the non-selected control population. X-axis represents a random distribution of the genes. **b,** E2 protein expression in control or ΔFHL1 cells infected with the CHIKV 21 strain (MOI of 10)**. c,** ΔFHL1 HAP1 cells were trans-complemented with FHL1A, B or C isoforms, infected with CHIKV 21 strain (MOI of 10) and stained for E2 protein expression at 48hpi. Data shown in **b** and **c** are mean +/- SD (3 experiments, n=6; one-way ANOVA with Dunnett's multiple comparisons test). **d,** ΔFHL1 and control cells were inoculated with CHIKV-Ross (MOI of 10), CHIKV-Brazza (MOI of 10), CHIKV-20235 (MOI of 10), CHIKV-M (M-899) (MOI of 10) or CHIKV-37997 (MOI of 10) and analyzed at 24 (293T) or 48hpi (HAP1) for E2 expression. Data shown are mean +/- SD (4 experiments, n=8 excepted for CHIKV-37997 n=4; one-way ANOVA with Tukey's multiple comparisons test). **e-g,** ΔFHL1 and control HAP1 cells were inoculated with O'nyong-nyong virus (ONNV) (MOI of 2), Mayaro virus (MAYV) (MOI of 50), Eastern equine encephalitis virus (EEEV) (MOI of 2), Sindbis virus (SINV), Semliki Forest Virus (SFV), Ross River virus (RRV), Western equine encephalitis virus (WEEV), Venezuelan equine encephalitis virus (VEEV), Dengue virus (DENV) (MOI of 0.4) or ZIKA virus (ZIKV) (MOI of 50). **e,** Infection was quantified 48hpi by flow cytometry using the anti-E2 3E4 or 265 CHIKV mAb or the anti-EEEV mAb 1A4B6 (2 experiments, n=4). **f,** Virus growth was assessed at day 4 pi using real-time RT-PCR. Serial dilutions of infected supernatants titrated using the TCID50 method were used as quantification standards for RT-PCR. Accordingly, results were expressed for each virus as "molecular equivalents of TCID50"**.** Data

shown are representative of two experiments. **g,** DENV or ZIKV infection were assessed by flow cytometry 48hpi using the anti-E protein 4G2 mAb. (3 experiments, n=6). **e-g** Data shown are mean +/- SD and significance was calculated using a one-way ANOVA statistical test with a Tukey's multiple comparisons test. **h,** BeWo and HepG2 cells were transduced with FHL1A or a control vector and challenged with CHIKV21 (MOI of 5) or CHIKV- M-899 (MOI of 2). Infection was quantified two days later by flow cytometry using the 3E4 mAb. Data shown are mean +/- SD (2 experiments, n=4 excepted for BeWo cells infected with CHIKV21, 3 experiments, n=6; one-way ANOVA with Tukey's multiple comparisons test). n.s non-significant; *** p< 0.0001.

Figure 2. FHL1 interacts with CHIKV nsP3 and is required for CHIKV RNA replication

a, Control and ΔFHL1 HAP1 cells were inoculated with CHIKV 21 (MOI of 10). At the indicated time points, cells were treated with trypsin to remove cell surface bound virus and viral RNA was quantified by qRT-PCR. Data shown are mean +/- SD (3 experiments, n=9; two-tailed t-test). **b**, Control or ΔFHL1 293T cells were transfected with *in vitro* transcribed CHIKV-M RNA expressing gaussia luciferase (Gluc) and Gluc activity was monitored at the indicated time points. RLU, relative light units. Data shown are mean +/- SEM (3 experiments, n=12; multiple t-tests). **c,** Control or ΔFHL1 293T cells were transfected with a replication-deficient mutant CHIKV (CHIKV-GAA) RNA expressing renilla luciferase (RLuc) and luc activity was monitored at the indicated time points. Data shown are mean +/- SEM (3 experiments, n=12; multiple t-tests). **d,** Control or ΔFHL1 293T cells were transfected with a replication-competent (CHIKV-GDD) or a replicon-deficient mutant CHIKV (CHIKV-GAA) capped RNA

893 expressing RLuc . The Rluc activity was monitored at described in c. Data shown are
894 mean +/- SEM (3 experiments, n=12; 2-way ANOVA with Tukey's multiple comparison
895 test). **e,** negative stranded viral RNA quantification by qRT-PCR from samples
896 collected in (**a)**. Data shown are mean +/- SD (2 experiments, n=8; one-way ANOVA
897 with a Tukey's multiple comparisons test). Dashed line represents the experimental
898 background threshold. **f,** Control and ΔFHL1 293T cells were inoculated with CHIKV
899 21 (MOI of 50). (left panel) Representative images of infected cells stained with anti-
900 dsRNA mAb at 6hpi. (right panel) Number of foci per cell was quantified using the Icy
901 software (2 experiments, n=42 cells in control and n=45 cells in ΔFHL1 cells; two-tailed
902 t-test). **g,** Transmission electron microscopy of control and ΔFHL1 HAP1 cells
903 challenged with CHIKV21 (MOI of 100) at 24h post-infection. Left panel shows CPV-II
904 structures containing attached nucleocapsids at their cytoplasmic side (white arrows)
905 as well as viral particles at the cell surface (thin black arrows). Middle panels show
906 replication spherules (arrowheads) together with viral particles (thin black arrows) at
907 the plasma membrane. PM= Plasma membrane. (Bars, 200nm). **h,** Co-
908 immunoprecipitation of endogenous FHL1 and CHIKV nsP3 from cell lysates of 293T
909 cells infected with a CHIKV nsP3-mCherry reporter virus at MOI 5 or 50. **i,** *In vitro* co-
910 immunoprecipitation analyzing the direct interaction between CHIKV-nsP3 and FHL1A
911 through the HVD domain. GST-precipitation of GST-nsP3 or GST-nsP3ΔHVD and
912 immunoblot analysis of 6xHis-FHL1A. **j, 2**93 T were co-transfected with plasmids
913 encoding FHL1A-HA and FLAG-tagged CHIKV nsP3 WT or CHIKV nsP3 ΔHVD or
914 CHIKV lacking the amino acid region 423-454 (ΔR4). Cellular lysates were subject to
915 immunoprecipitation with anti-FLAG beads followed by immunoblot analysis with anti-
916 FLAG or anti-HA mAb. **k,** (left panel) Schematic representation of FHL1A protein in
917 fusion with the nsP3 interacting region (FHL1A-R4) or a similar randomized sequence

(FHL1A-R4*). (Right panel) Immunoassay of the interaction between CHIKV nsP3 and FHL1A fusion proteins in 293T cells co-transfected with FLAG-tagged CHIKV nsP3 and either a HA-tagged FHL1A, FHL1A-R4 or FHL1A-R4* constructs. Cellular lysates were subject to immunoprecipitation with anti-FLAG followed by immunoblot analysis with anti-FLAG and anti-HA Ab. **l,** ΔFHL1 293T cells were transfected with an empty vector or plasmids encoding FHL1A, FHL1A-R4 or FHL1A-R4*. Cells were incubated with CHIKV21 (MOI of 5) and infection was quantified 24hpi by flow cytometry. Data shown are mean +/- SD (2 experiments, n=4; one-way ANOVA with Dunnett's multiple comparison test). ** P< 0.01 **** P< 0.0001; ns not significant.

Figure 3. Primary myoblasts and fibroblasts from FHL1 deficient patients are resistant to CHIKV infection.

a, FHL1 expression in primary myoblasts and fibroblasts from healthy donors or Emery-Dreifuss muscular dystrophy (EDMD) patients. CM: control myoblasts, PM: patient myoblasts; CF: control fibroblast, PF: patient fibroblasts. **b,** Cells from controls or EMDM patients were inoculated with CHIKV expressing nsP3-mCherry. At 48-hpi, cells were fixed and images were taken on fluorescence microscope. Images are representative of three experiments. **c,** E2 protein expression in primary cells from healthy controls or EDMD patients infected with CHIKV21 (MOI of 2). Data shown are mean +/- SD (2 experiments, n=4 for myoblast; 4 experiments, n=8 for fibroblast; one-way ANOVA with Tukey's multiple comparisons test). **d,** Quantification of viral particles released in supernatant of infected cells collected at 24, 48- and 72-hpi. FIU, flow cytometry infectious units. Data shown are mean +/- SEM (2 experiments, n=4 for myoblast; 3 experiments, n=6 for fibroblast; multiple t-test). **e,** Primary fibroblasts from a control (CF1) or two FHL1 null patients (PF2, PF4) were inoculated with CHIKV-

Ross, CHIKV-Brazza, CHIKV-H20235 strains or MAYV (MOI of 2) and analyzed for E2 expression. Data shown are mean +/- SD (3 experiments n=6, one-way ANOVA with Dunnett's multiple comparisons test). **f**-**g** Fibroblasts from control (CF1) or FHL1 null patients (PF2, PF4) were transduced with a lentiviral vector encoding FHL1A or a control vector and then challenged with CHIKV21 (MOI of 2). **f,** Infection was quantified as described in c. Data shown are mean +/- SD (2 experiments, n=4, one-way ANOVA with Tukey's multiple comparisons test). **g**, Supernatants were collected from infected cells at indicated time point and viral titers were measured on VeroE6 cells. Data shown are mean +/- SEM (2 experiments, n=4; two-way ANOVA with Dunnett's multiple comparisons test). *P<0.05; **P<0.01; **** P< 0.0001; ns not significant.

Figure 4. FHL1 is a factor of susceptibility to CHIKV infection in mice.

a, Viral titers in tissues of nine-day-old mice. WT littermates (n=5) and FHL1-null mice (n=7) were inoculated with 10^5 PFU of CHIKV via the ID route and sacrificed by 7 days post infection. The amount of infectious virus in tissues was quantified by TCID50. The broken line indicates the detection threshold. **b,** Hematoxylin and eosin staining of transversal section of skeletal muscle in CHIKV-infected mice. **c,** Immunostaining of nuclei, FHL1, vimentin and CHIKV antigens on skeletal muscle of CHIKV-infected mice. ** P<0.01; ns not significant.

Extended Data Figures

Extended Data Fig. 1. CRISPR-Cas9 genetic screen identified essential host factors of CHIKV infection

a, Schematic of CRISPR-Cas9 genome-wide screen in HAP1 haploid cells. **b**, Ranked list of the top 30 genes identified using MAGeCKs algorithm and their corresponding rank in RIGER analysis. **c**, Venn diagram comparing the top 200 hits from our screen and previous CRISPR and haploid screens for CHIKV host factors.

Extended Data Fig. 2. Validation of FHL1 gene edition by CRISPR-Cas9

Schematic of the genomic organization of FHL1 **(a)**, alternative splicing of the isoforms FHL1A, FHL1B and FHL1C **(b)** and their corresponding proteins **(c)**. Initiation and stop codon are indicated in red and relative positions of the sequence targeted by the sgRNA are indicated in blue. **d**, Sanger sequencing of FHL1 in control and ΔFHL1 HAP1 cells. **e**, Genomic DNA was used for PCR amplification using primers flanking the sequence targeted by FHL1 sgRNA2. The absence of an amplification product of 3.9 kb (black arrow) in HAP1 clone suggests that a large indel is responsible for the absence of FHL1 expression. Asterisk: unspecific PCR products. **f,** Immunoblot of FHL1 in control and ΔFHL1 cells. One representative of three experiments is shown. **e**, Control and ΔFHL1 cells were plated and viability was assessed over a 72 hours period using the CellTiter-Glo assay. Data shown are mean +/- SEM (2 experiments, n=8; two-way ANOVA with Dunnett's multiple comparisons test). *P<0.05; ns not significant.

Extended Data Fig. 3. FHL1 is an essential host factor for CHIKV and ONNV infection

a, Immunofluorescence images of control and ΔFHL1 HAP1 cells inoculated with CHIKV21 (MOI of 10), fixed 48 hpi and stained for E2 expression. **b,** Immunofluorescence images of control and ΔFHL1 HAP1 cells inoculated with CHIKV expressing nsP3-mCherry (MOI of 10) and fixed 48 hpi. **a, b,** Images were taken on fluorescence microscope and are representative of three experiments. **c**, Control and ΔFHL1 HAP1 cells were inoculated with increasing MOI of CHIKV21, and infection was quantified 48hpi by flow cytometry using the anti-E2 3E4 mAb. Data shown are mean +/- SD (3 experiments, n=6; two-way ANOVA with Tukey's multiple comparison test). **d,** Multi-step growth curves with CHIKV 21 strain in control or ΔFHL1 cells. Data shown are mean +/- SEM (2 experiments, n=4; multiple t-tests). **e,** Control and ΔFHL1 HAP1 cells were inoculated with increasing MOI of ONNV or MAYV, and Infection was quantified 48hpi by flow cytometry using anti-E2 3E4 and 265 mAbs. Data shown are mean +/- SEM (2 experiments, n=4; two-way ANOVA with Tukey's multiple comparisons test). **f**, Control and ΔFHL1 HAP1 cells were inoculated with increasing MOI of DENV or ZIKV, and infection was quantified 48hpi by flow cytometry using the anti-E 4G2 mAb. Data shown are mean +/- SEM (3 experiments, n=6; two-way ANOVA with Tukey's multiple comparisons test). * P< 0.05; **** P< 0.0001; ns not significant.

Extended Data Fig. 4. FHL1A and FHL2 ectopic expression in ΔFHL1 cells restores CHIKV infection

a, Immunoblot of ectopic FHL1 expression in HAP1 cells stably transduced with an empty vector or FHL1A, FHL1B or FHL1C isoform. **b,** Quantification in the supernatant

of infected HAP1 cells of viral particles released by measuring viral titer on Vero E6 cells. Data shown are representative of 3 experiments, mean +/- SEM. **c,** ΔFHL1 293T cells transfected with an empty vector or HA-tagged plasmids encoding FHL1A and FHL2 were subjected to infection with increasing MOI of CHIKV21. Infection was quantified 24hpi by flow cytometry. Data shown are mean +/- SD (3 experiments, n=6; two-way ANOVA with Dunnett 's multiple comparison test) **P<0.01; **** P< 0.0001; ns not significant.

Extended Data Fig. 5. FHL1A overexpression in BeWo and HepG2 cells enhances CHIKV infection

a, Expression of endogenous FHL1 in HAP1, 293T, BeWo and HepG2. **b,** Immunoblot of ectopic FHL1 expression in Bewo and HepG2 cells stably transduced with an empty vector or HA-tagged FHL1A. **c** and **d,** Bewo cells stably transduced with an empty vector or HA-tagged FHL1A were inoculated with increasing MOI of CHIKV21. **c,** Infection was quantified 48hpi by flow cytometry using the anti-E2 3E4 mAb. Data shown are mean +/- SEM (3 experiments, n=6; Two-way ANOVA with Tukey's multiple comparisons test). **d,** Quantification in the supernatants of infected cells of viral particles released by measuring viral titer on Vero E6 cells. Data shown are mean +/- SD (2 experiments, n=4; two-tailed t-test). **e,** HepG2 cells stably transduced with an empty vector or FHL1A were inoculated with increasing MOI of CHIKV-M-Gluc. Infection was quantified 48hpi as indicated in c. Data shown are mean +/- SEM (2 experiments, n=4; Two-way ANOVA with Tukey's multiple comparisons test). ** P<0.001; **** P< 0.0001; ns not significant.

Extended Data Fig. 6. CHIKV nsP3 directly interacts with FHL1A and FHL2

a, Control or ΔFHL1 HAP1 cells were transfected with CHIKV-M-Gluc capped genomic RNA expressing Gaussia luciferase (Gluc). Gluc activity was monitored at indicated time point. RLU, relative light units. Data shown are mean +/- SEM (3 experiments, n=12; multiple t-tests). **b,** Confocal microscopy of the colocalization of CHIKV nsP3 with FHL1 protein in fibroblasts inoculated with CHIKV-nsP3-mCherry (MOI of 2), fixed 48 hpi and stained with anti-FHL1. Images are representative of three experiments. **c,** Immunoassay of the interaction between CHIKV nsP3 and FHL1 isoforms in 293T cells transfected with FLAG-tagged CHIKV nsP3 and either an empty vector or plasmids encoding the three HA-tagged FHL1 isoforms. Cellular lysates were subject to immunoprecipitation with anti-FLAG followed by immunoblot analysis with anti-FLAG and anti-HA. **d,** Immunoassay of the interaction between CHIKV nsP3 and FHL2 in 293Tcells transfected with FLAG-tagged CHIKV nsP3 and either an empty vector or plasmids encoding HA-tagged FHL1 and FHL2. Cellular lysates were subject to immunoprecipitation with anti-FLAG followed by immunoblot analysis with anti-FLAG and anti-HA. **e,** Endogenous FHL1, G3BP1 or G3BP2 immunoprecipitation from control and ΔFHL1 293T cells transfected with plasmids encoding FLAG-tagged CHIKV, Sindbis (SINV) or Semliki forest virus (SFV) nsP3. Cellular lysates were subject to immunoprecipitation with anti-FLAG followed by immunoblot analysis with anti-FLAG, anti-FHL1, anti-G3BP1 and anti-G3BP2. **f,** Endogenous FHL1 immunoprecipitation from 293T cells transfected with plasmids encoding FLAG-tagged full length CHIKV nsP3, CHIKV nsP3 carrying the SINV HVD (CHIKV/HVD-SIV) or Sindbis nsP3 carrying CHIKV HVD (SINV/HVD-CHIKV). Cellular lysates were subjected to immunoprecipitation with anti-FLAG followed by immunoblot analysis with anti-FLAG and anti-FHL1. **g,** Purified GST-tagged nsP3 constructs and HA-tagged

FHL1A detected by coomassie blue staining. **c-i,** One experiment representative of three is shown. *P<0.05; **P<0.01; **** P< 0.0001; ns not significant.

Extended Data Fig. 7. Mapping the FHL1–nsP3 interaction

a, The sequence alignment of nsP3 protein HVD domains of representative members of New and Old World alphaviruses. Sequence alignment was performed with Clustall Omega and edited with Jalview. R1, R2 and R3 sequences of high homology between CHIKV strains and ONNV are defined by colored lines. CHIKV06-21 (GenBank accession number AM258992.1); CHIKV Ross (GenBank accession number MG280943.1); CHIKV H20235 (GenBank accession number MG208125.1); CHIKV 37997 (GenBank accession number AY726732.1); ONNV (GenBank accession number MF409176.1); SFV (GenBank accession number HQ848388.1); MAYV (GenBank accession number KY618137.1); SINV (GenBank accession number MF409178.1); EEEV (GenBank accession number Q4QXJ8.2); VEEV (GenBank accession number P27282.2). **b,** (top panel) Schematic representation of CHIKV nsP3 constructs deleted for the R1, R2, R3 or R4 sequences. (bottom panel) 293T cells were transfected with FHL1A-HA and either an empty vector or plasmids encoding FLAG-tagged nsP3 constructs. Cell lysates were immunoprecipitated with anti-FLAG followed by immunoblot analysis with anti-HA or anti-FLAG Ab. One experiment representative of three is shown. **c,** Alignment of nsP3 regions containing the WT R4 sequence or the corresponding randomized sequence. Dashes represents identical aa. **d,** Control 293T cells were transfected with the indicated CHIKV capped in vitro transcribed RNA expressing renilla luciferase (Rluc). Rluc activity was monitored at indicated time points. RLU, relative light units. Data shown are mean +/- SEM (2

experiments, n=8; Two-way ANOVA with Tukey's multiple comparisons test). **** P< 0.0001; ns not significant.

Extended Data Fig. 8. CHIKV Infection of myoblasts and fibroblasts derived from EDMD patients

a, Schematic of FHL1A protein in three EDMD patient (P1, P2 and P3). **b,** Schematic of FHL1 genomic organization in newly described patient with a LINE1 insertion within exon 4 (P4). **c,** Myoblasts and fibroblasts from EDMD patients or healthy donors were infected with increasing MOI of CHIKV21, and infection was quantified 24hpi by flow cytometry using the anti-E2 3E4 mAb. Data shown are mean +/- SEM (2 experiments, n=4 for myoblast; 3 experiments, n=6 for fibroblast; Two-way ANOVA with Dunnett's multiple comparisons test). **d**, Fibroblasts from EDMD patients or healthy donors were inoculated with increasing MOI of CHIKV-Ross, CHIKV-Brazza, CHIKV-H20235, and infection was quantified 24hpi by flow cytometry using the anti-E2 3E4 mAb. Data shown are mean +/- SEM (3 experiments, n=6; two-way ANOVA with Dunnett's multiple comparisons test). **e,** Immunoblot of ectopic FHL1 expression in patient primary fibroblast (PF2 and PF4) cells stably transduced with an empty vector or a plasmid encoding HA-FHL1A. One representative of two experiments is shown. **** P< 0.0001; ns not significant.

Extended Data Fig.9. Mouse FHL1 interacts with CHIKV nsP3 and restores infection in ∆FHL1 cells

a, Sequence alignment of murine and human FHL1A proteins. **b,** 293Tcells were co-transfected with FLAG-tagged CHIKV nsP3 and plasmids encoding HA-tagged mFHL1 or hFHL1A. Cellular lysates were subject to immunoprecipitation with anti-HA followed

by immunoblot analysis with anti-FLAG (nsP3) and anti-HA (FHL1). **c,** Immunoblot of FHL1 ectopic expression in ΔFHL1 293T stably transduced with plasmid encoding murine FHL1 (mFHL1) or human FHL1A (hFHL1A). **d,** Cells showed in **c** were inoculated with increasing MOI of CHIKV21. Infection was quantified by flow cytometry at 24 hpi using anti-E2 3E4 mAb. Data shown are mean +/-SD (3 experiments, n=6; two-way ANOVA with Dunnett's multiple comparisons test). **e,** (left panel) Immunoblot of endogenous FHL1 in control and ΔFHL1 C2C12 murine cells. (right panel) Control and ΔFHL1 cells were inoculated with CHIKV21 or MAYV (MOI of 2) and infection was quantified at 24hpi by flow cytometry using anti-E2 3E4 or anti-E2 265 mAb. One representative of three experiments is shown. ***P<0.001; ****P<0.0001; ns not significant.

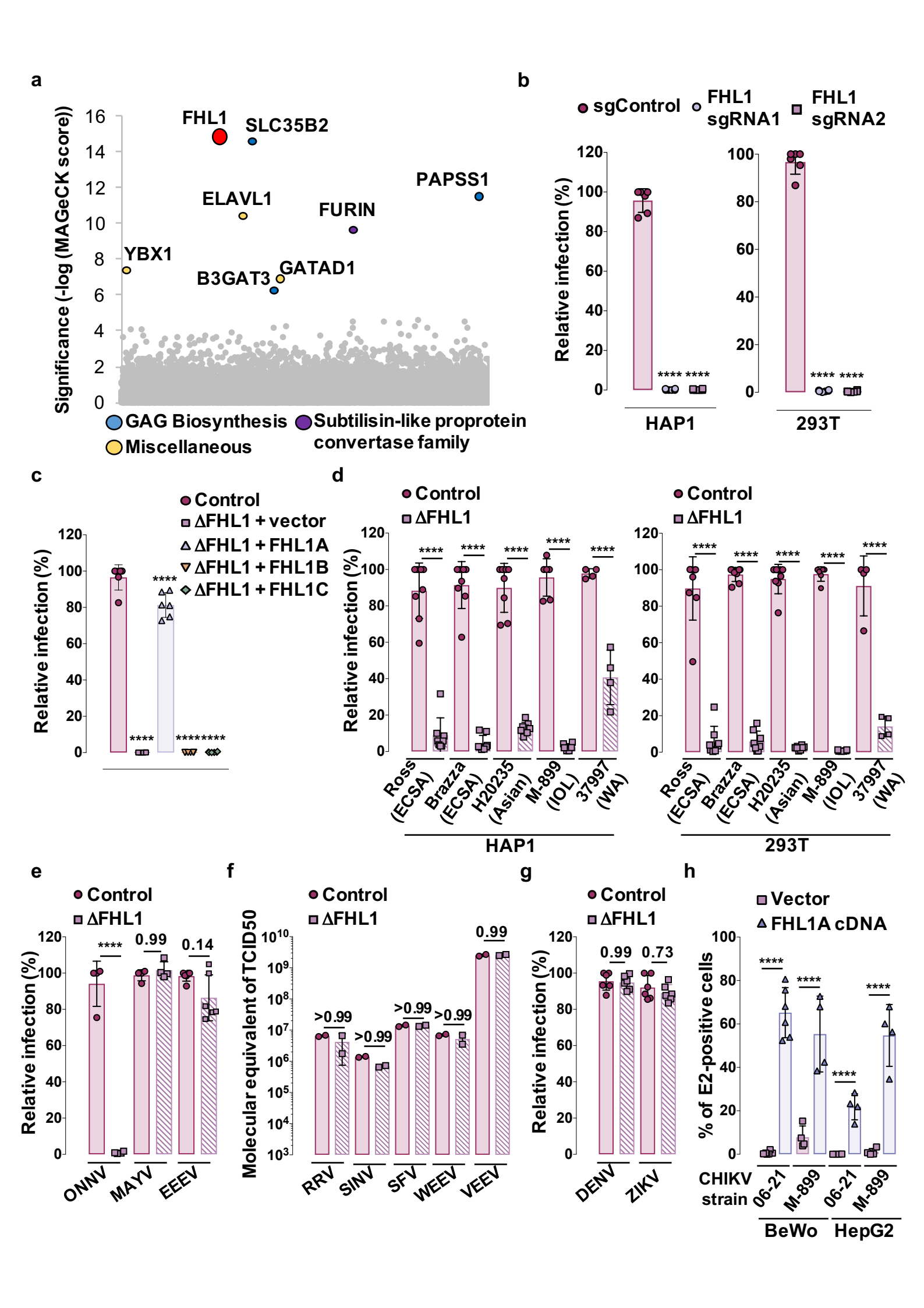
a
Significance (-log (MAGeCK score))
FHL1
SLC35B2
PAPSS1
ELAVL1
FURIN
YBX1
GATAD1
B3GAT3
GAG Biosynthesis
Subtilisin-like proprotein convertase family
Miscellaneous
b
sgControl
FHL1 sgRNA1
FHL1 sgRNA2
Relative infection (%)
HAP1
293T
c
Control
ΔFHL1 + vector
ΔFHL1 + FHL1A
ΔFHL1 + FHL1B
ΔFHL1 + FHL1C
Relative infection (%)
d
Control
ΔFHL1
Relative infection (%)
Ross (ECSA)
Brazza (ECSA)
H20235 (Asian)
M-899 (IOL)
37997 (WA)
HAP1
293T
e
Control
ΔFHL1
Relative infection (%)
0.99
0.14
ONNV
MAYV
EEEV
f
Control
ΔFHL1
Molecular equivalent of TCID50
>0.99
0.99
RRV
SINV
SFV
WEEV
VEEV
g
Control
ΔFHL1
Relative infection (%)
0.99
0.73
DENV
ZIKV
h
Vector
FHL1A cDNA
% of E2-positive cells
CHIKV strain
06-21
M-899
BeWo
HepG2

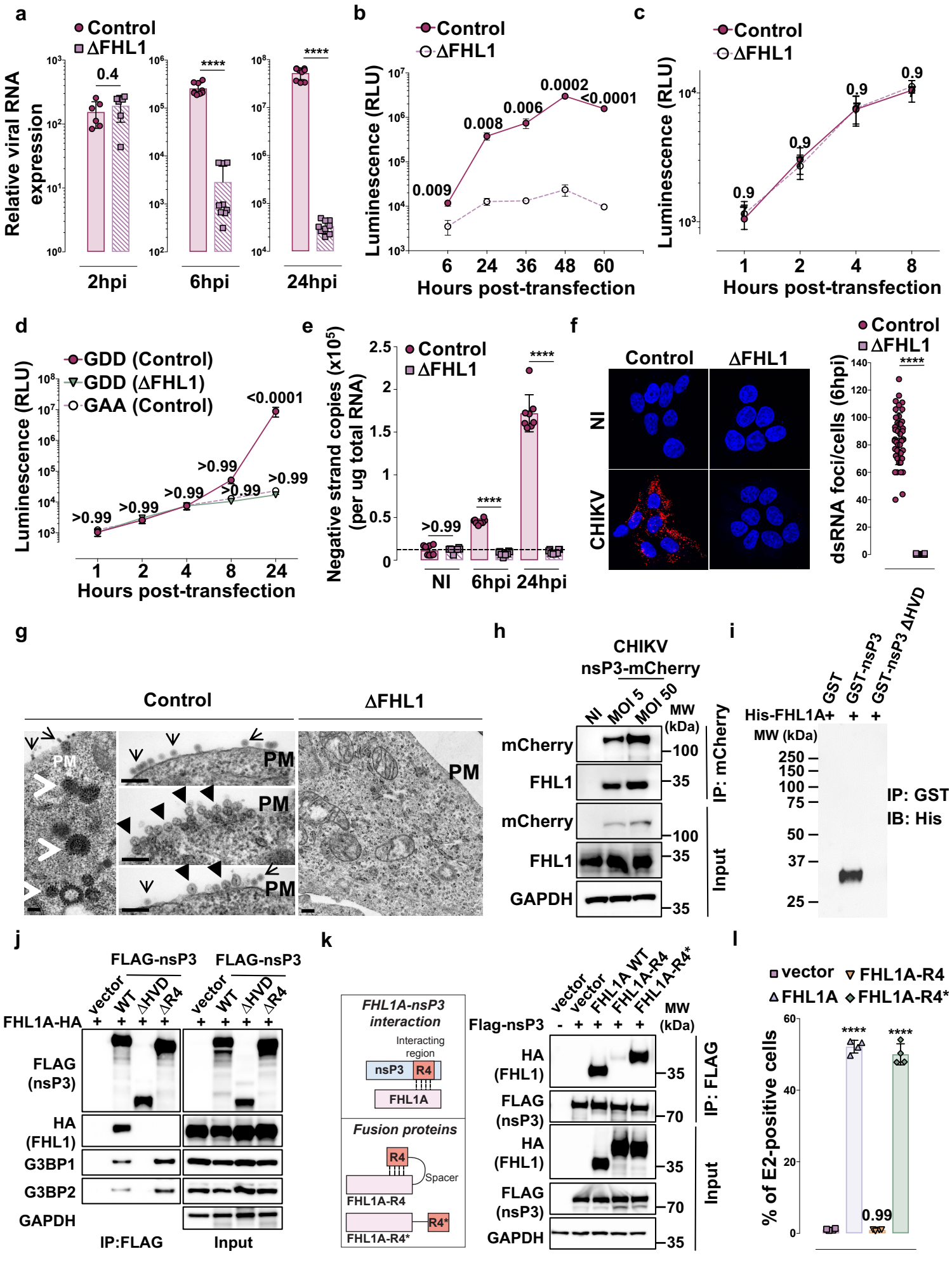
a
Control
ΔFHL1
Relative viral RNA expression
0.4
****
****
2hpi
6hpi
24hpi
b
Control
ΔFHL1
Luminescence (RLU)
0.009
0.008
0.006
0.0002
<0.0001
6 24 36 48 60
Hours post-transfection
c
Control
ΔFHL1
Luminescence (RLU)
0.9
0.9
0.9
0.9
1 2 4 8
Hours post-transfection
d
GDD (Control)
GDD (ΔFHL1)
GAA (Control)
Luminescence (RLU)
>0.99
>0.99
>0.99
>0.99
>0.99
<0.0001
1 2 4 8 24
Hours post-transfection
e
Control
ΔFHL1
Negative strand copies (x10^5) (per ug total RNA)
****
****
>0.99
NI
6hpi
24hpi
f
Control
ΔFHL1
NI
CHIKV
Control
ΔFHL1
dsRNA foci/cells (6hpi)
****
g
Control
ΔFHL1
PM
PM
PM
PM
PM
h
CHIKV nsP3-mCherry
NI
MOI 5
MOI 50
MW (kDa)
mCherry
FHL1
mCherry
FHL1
GAPDH
100
35
100
35
35
IP: mCherry
Input
i
GST
GST-nsP3
GST-nsP3 ΔHVD
His-FHL1A+
+
+
MW (kDa)
250
150
100
75
50
37
25
IP: GST
IB: His
j
FLAG-nsP3
FLAG-nsP3
vector
WT
ΔHVD
ΔR4
vector
WT
ΔHVD
ΔR4
FHL1A-HA
+ + + +
+ + + +
FLAG (nsP3)
HA (FHL1)
G3BP1
G3BP2
GAPDH
IP:FLAG
Input
k
FHL1A-nsP3 interaction
Interacting region
nsP3
R4
FHL1A
Fusion proteins
R4
Spacer
FHL1A-R4
R4*
FHL1A-R4*
vector
vector
FHL1A WT
FHL1A-R4
FHL1A-R4*
Flag-nsP3
- + + + +
MW (kDa)
HA (FHL1)
FLAG (nsP3)
HA (FHL1)
FLAG (nsP3)
GAPDH
35
70
35
70
35
IP: FLAG
Input
l
vector
FHL1A-R4
FHL1A
FHL1A-R4*
% of E2-positive cells
****
****
0.99
60
40
20
0

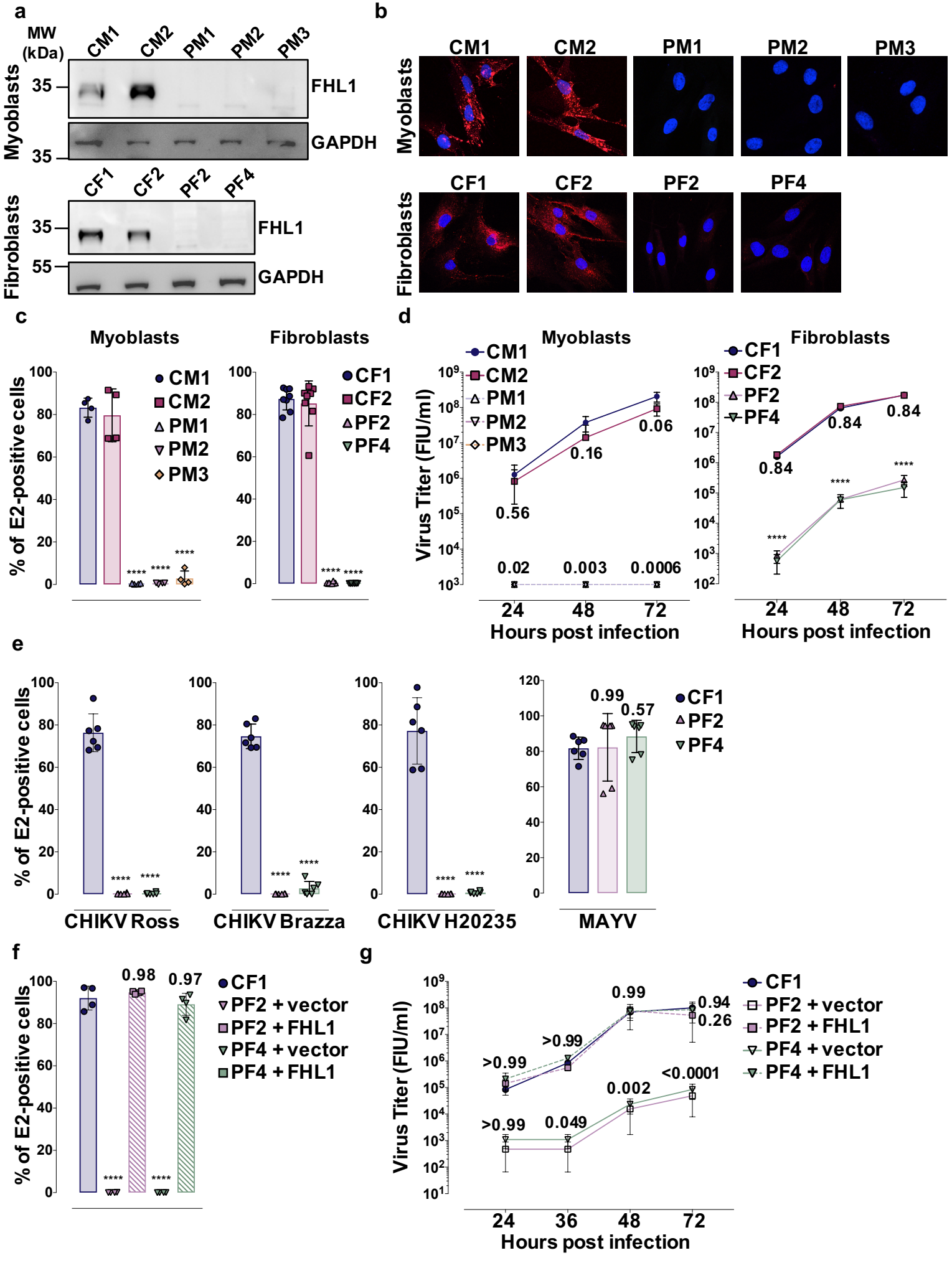
a
MW (kDa)
CM1
CM2
PM1
PM2
PM3
Myoblasts
35
FHL1
35
GAPDH
CF1
CF2
PF2
PF4
Fibroblasts
35
FHL1
55
GAPDH
b
CM1
CM2
PM1
PM2
PM3
Myoblasts
CF1
CF2
PF2
PF4
Fibroblasts
c
Myoblasts
Fibroblasts
% of E2-positive cells
CM1
CM2
PM1
PM2
PM3
CF1
CF2
PF2
PF4
****
d
Myoblasts
Fibroblasts
Virus Titer (FIU/ml)
CM1
CM2
PM1
PM2
PM3
CF1
CF2
PF2
PF4
0.56
0.16
0.06
0.02
0.003
0.0006
0.84
0.84
0.84
****
24
48
72
Hours post infection
e
% of E2-positive cells
CHIKV Ross
CHIKV Brazza
CHIKV H20235
MAYV
0.99
0.57
CF1
PF2
PF4
****
f
% of E2-positive cells
0.98
0.97
CF1
PF2 + vector
PF2 + FHL1
PF4 + vector
PF4 + FHL1
****
g
Virus Titer (FIU/ml)
0.99
0.94
0.26
>0.99
>0.99
<0.0001
0.002
>0.99
0.049
CF1
PF2 + vector
PF2 + FHL1
PF4 + vector
PF4 + FHL1
24
36
48
72
Hours post infection

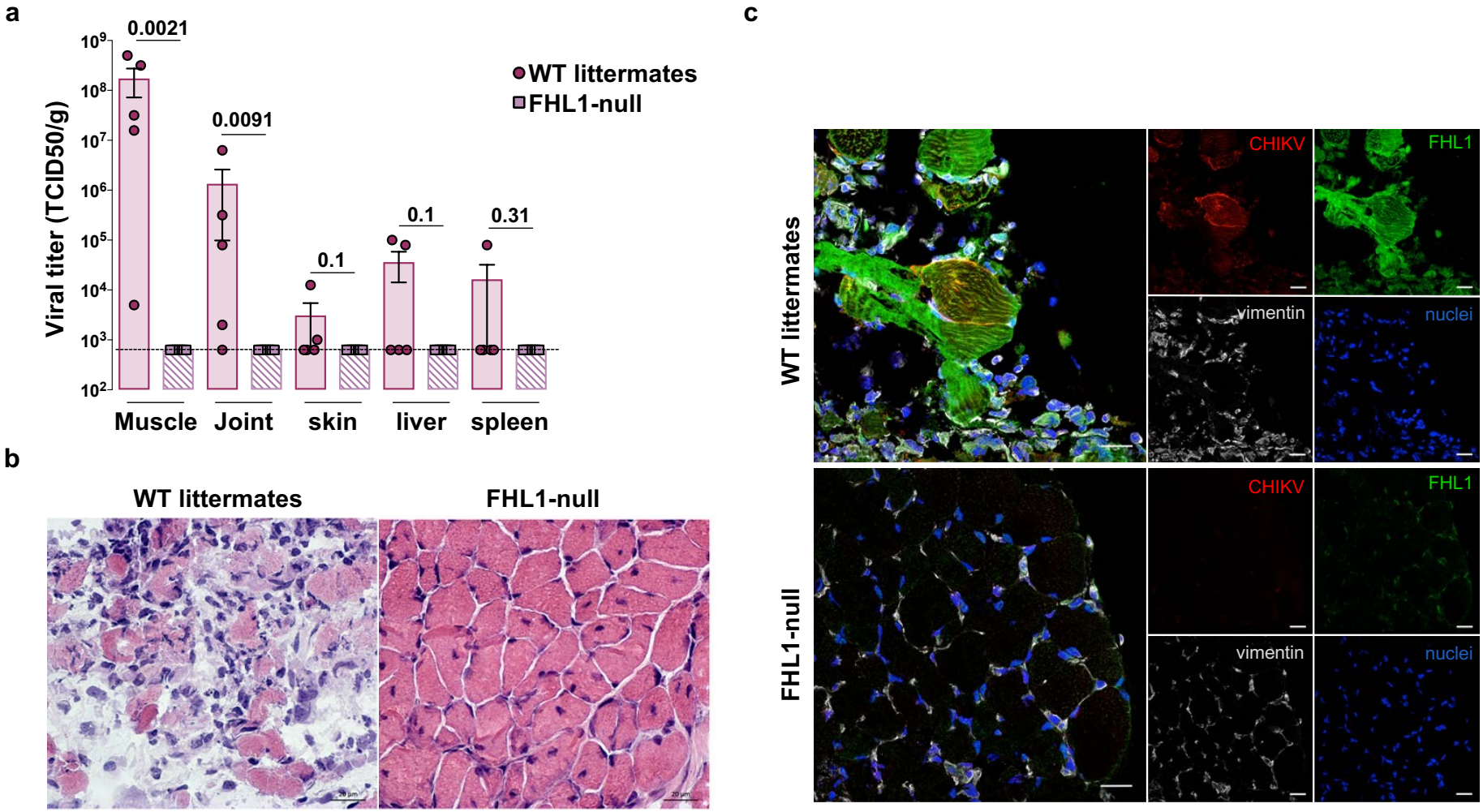
a
0.0021
0.0091
0.1
0.1
0.31
WT littermates
FHL1-null
Viral titer (TCID50/g)
Muscle
Joint
skin
liver
spleen
b
WT littermates
FHL1-null
c
WT littermates
FHL1-null
CHIKV
FHL1
vimentin
nuclei

a

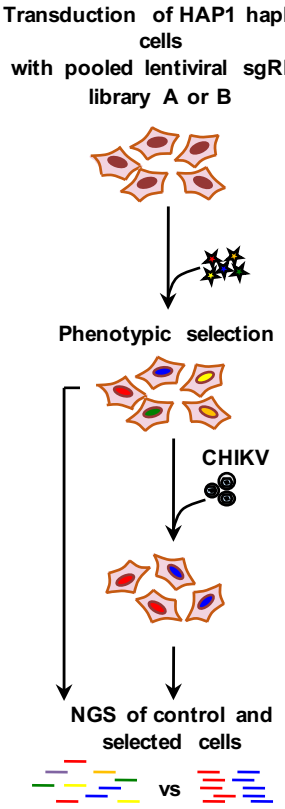

b

Ranked Genes	MAGeCK rank	RIGER Rank
FHL1	1	1
SLC35B2	2	2
PAPSS1	3	3
ELAVL1	4	4
FURIN	5	7
YBX1	6	6
GATAD1	7	5
B3GAT3	8	9
OR10W1	9	217
MTRNR2L5	11	18
COA5	12	436
POMT2	13	641
ELP5	14	47
PRIM2	16	337
NRCAM	17	238
PDE8B	18	78
EXT1	19	26
ELF2	20	10
MYT1L	21	381
CUL5	22	956
MAP4K3	23	37
ALDH18A1	24	107
ACTR10	25	13544
SLC7A6OS	26	2704
C11orf30	27	11
BID	28	8
SMOC1	30	507
SCGB1D1	32	84
RPE65	33	75
FAM124B	34	459

c

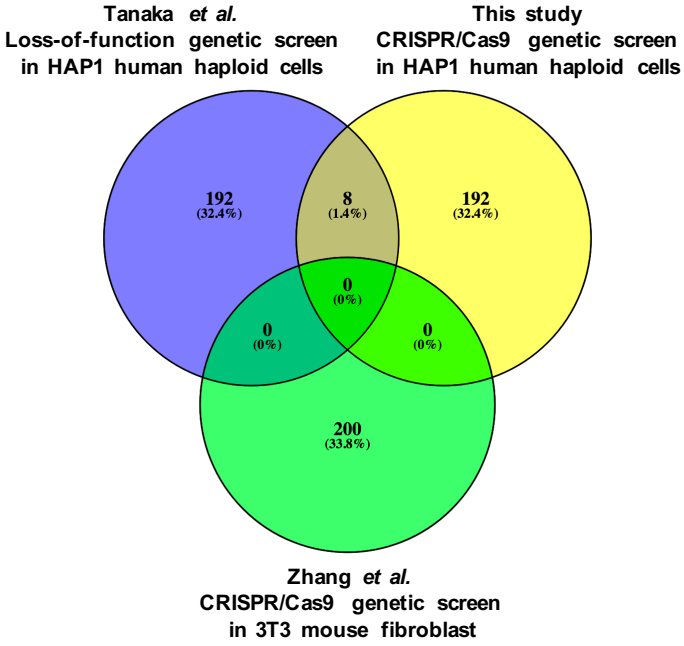

Extended Figure 1

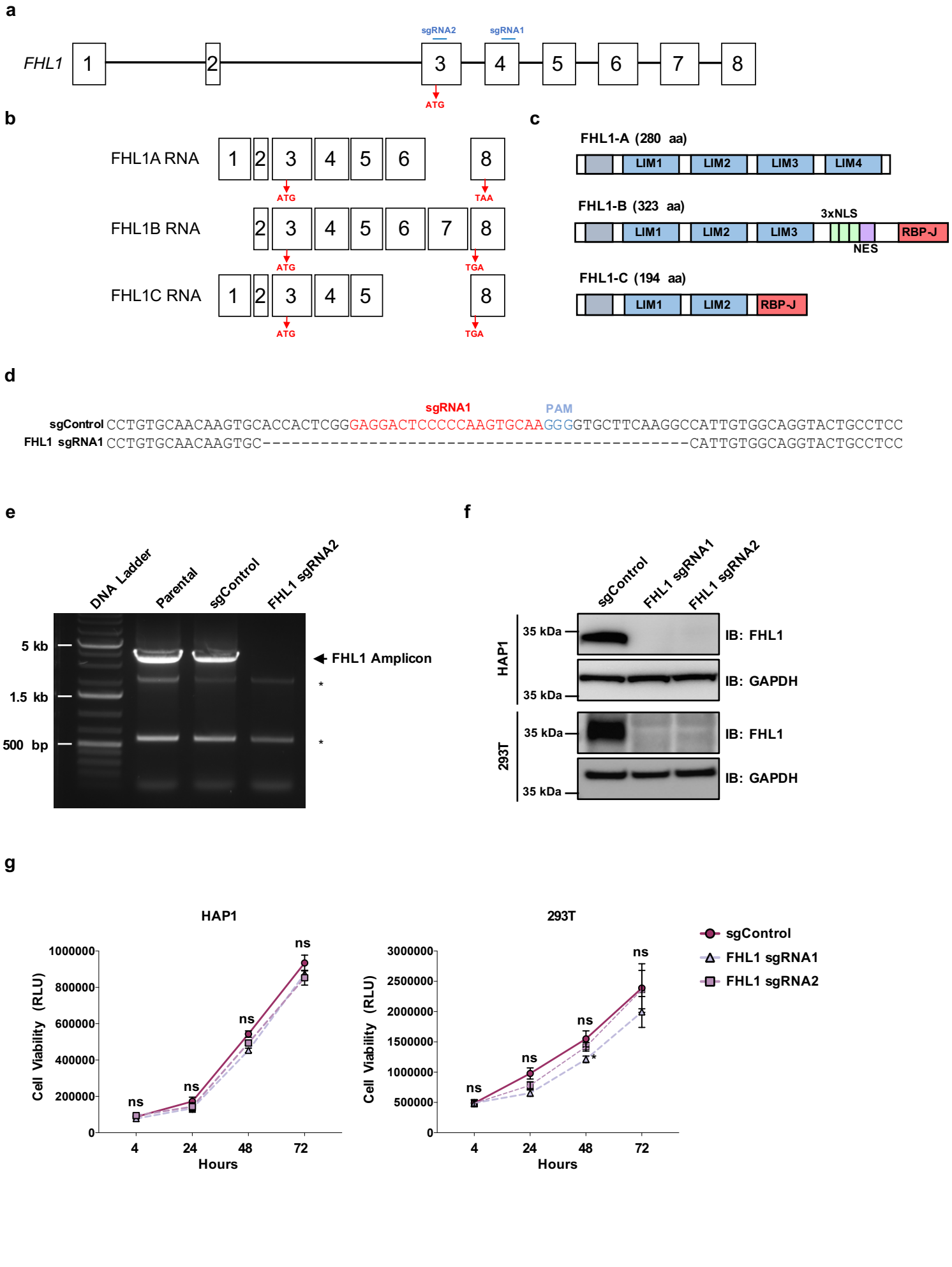

Extended Figure 2

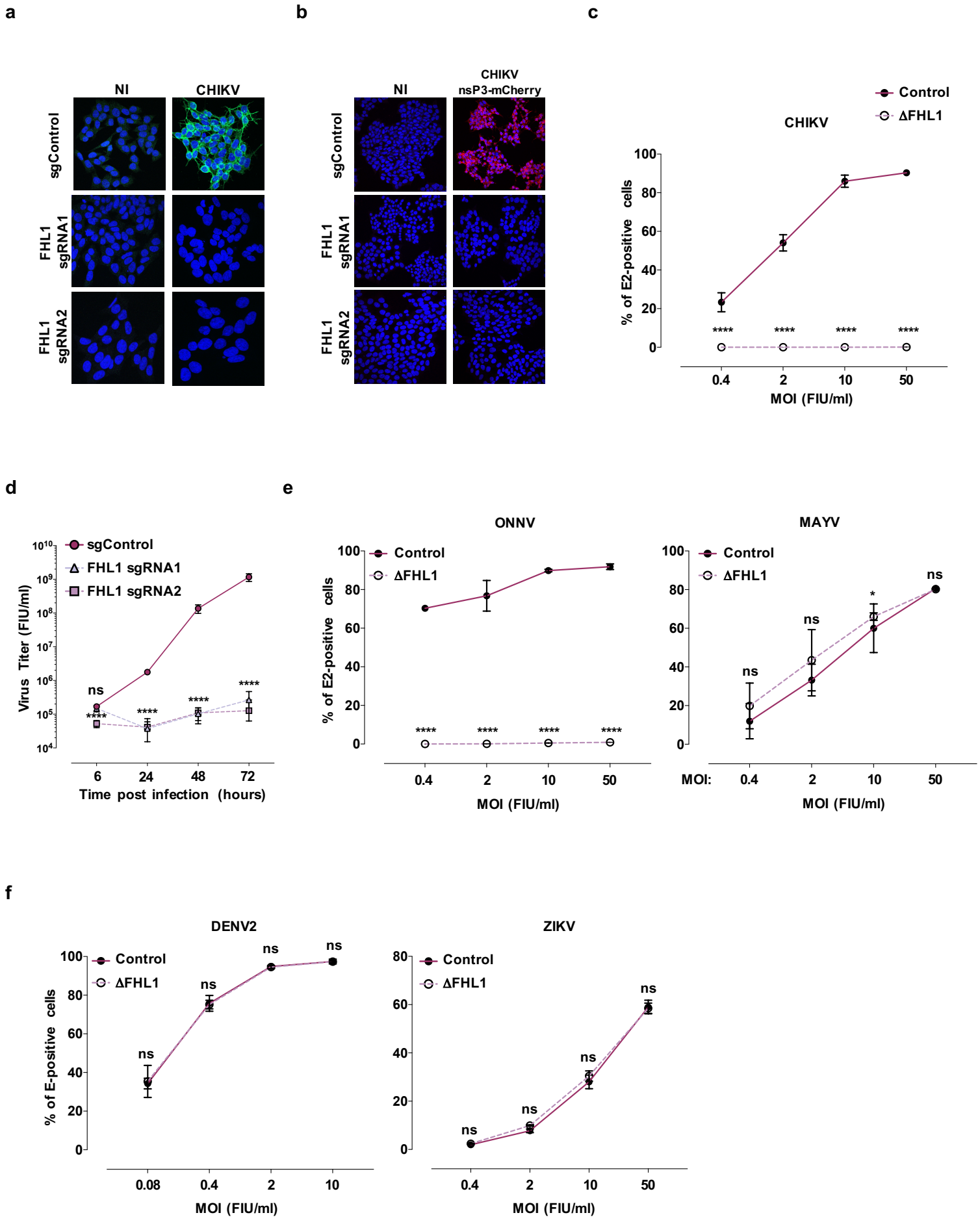

Extended Figure 3

a

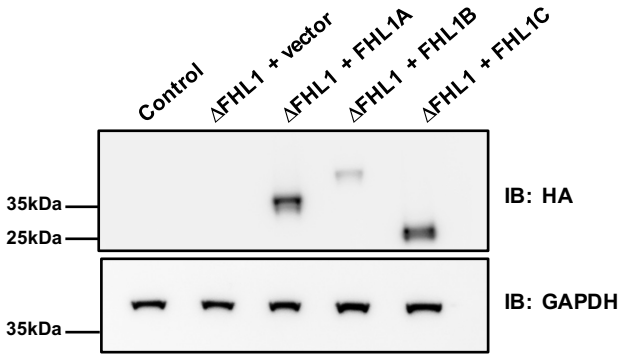

b

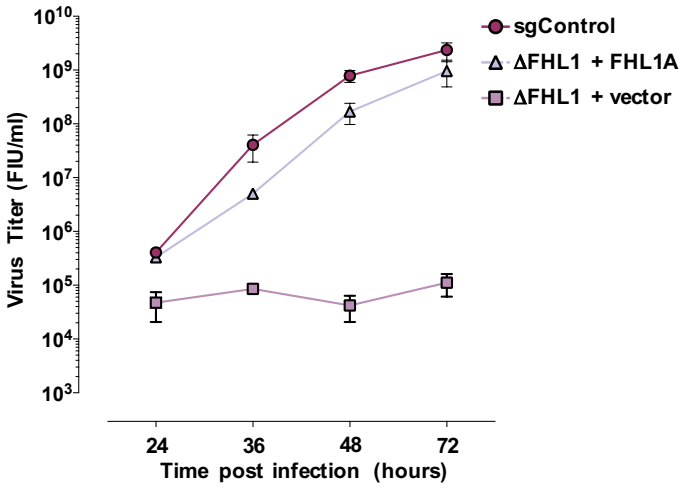

c

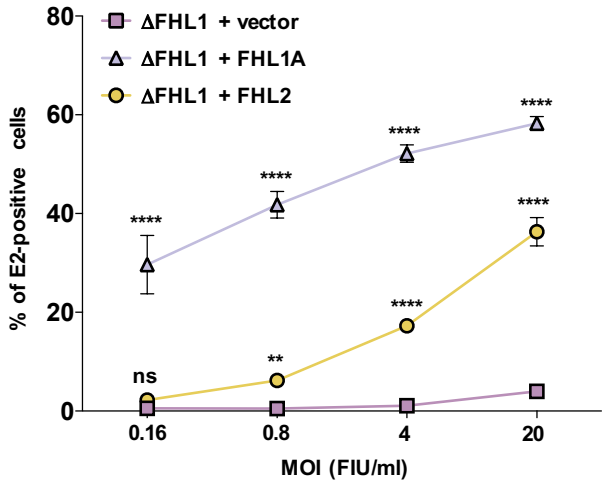

Extended Figure 4

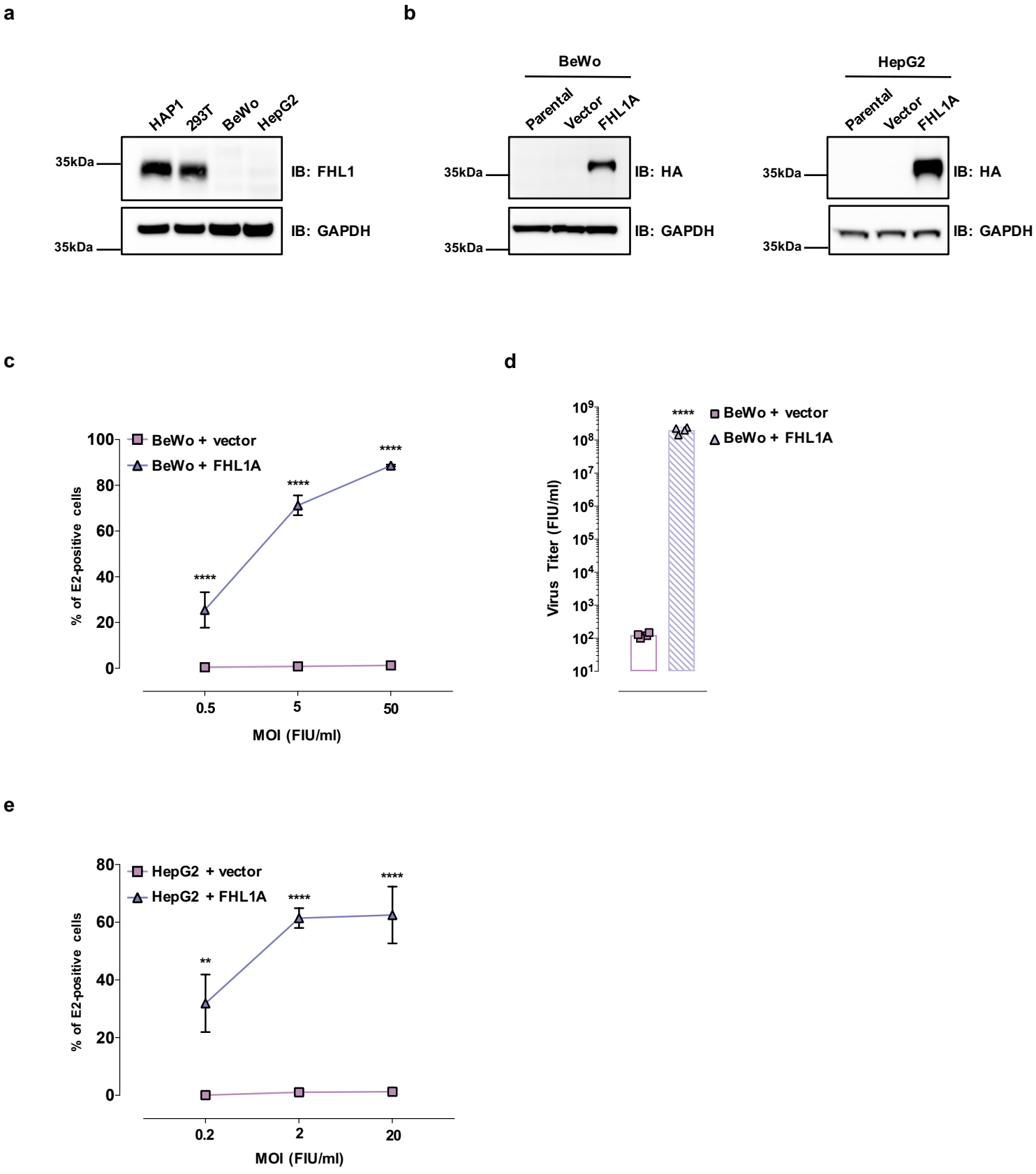

Extended Figure 5

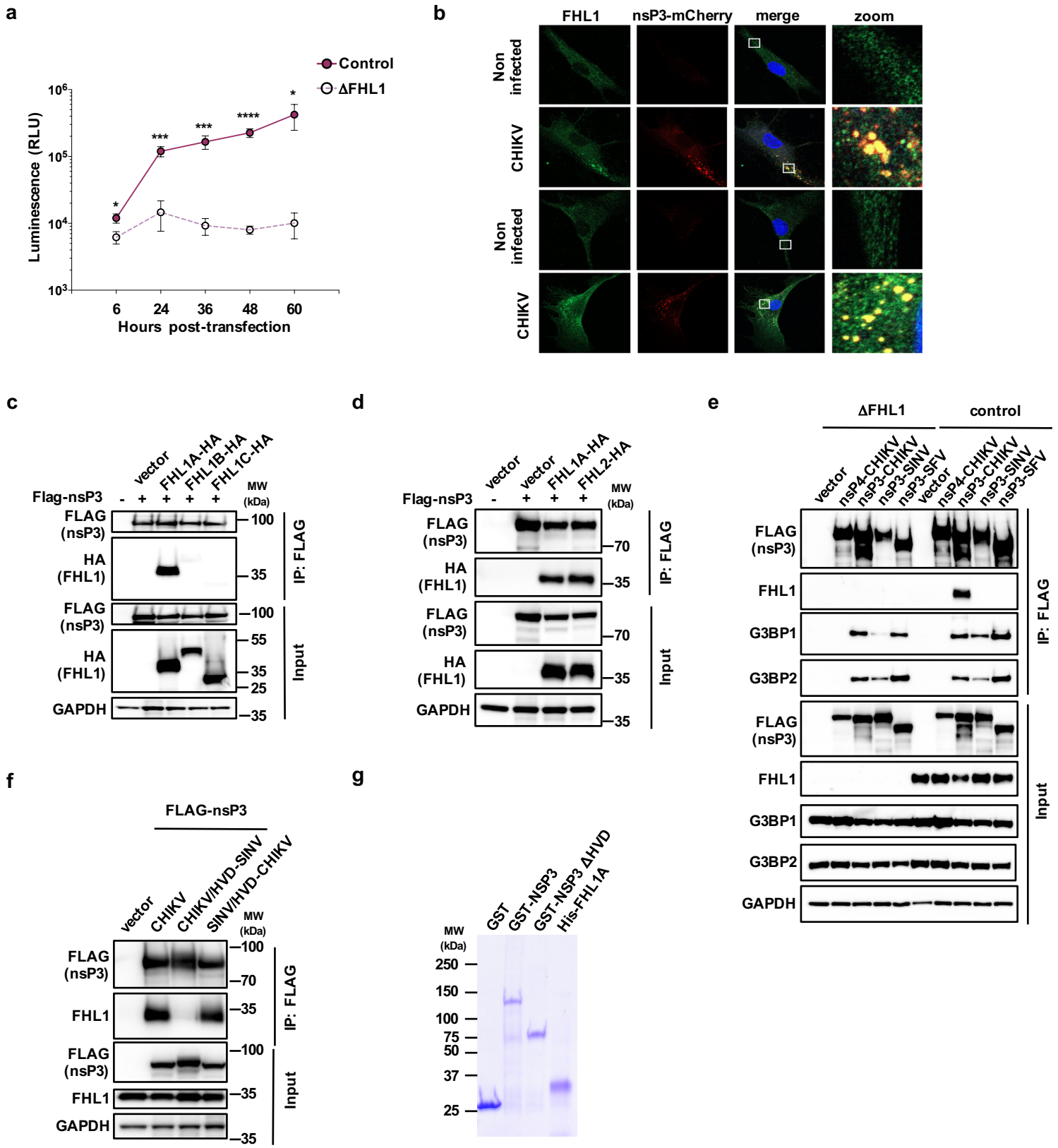

Extended Figure 6

a

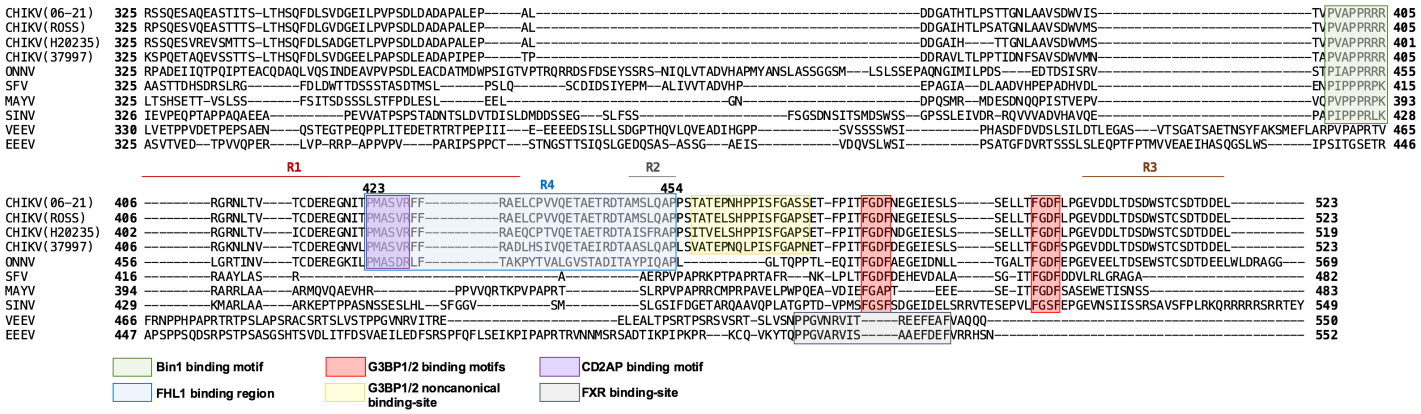

b

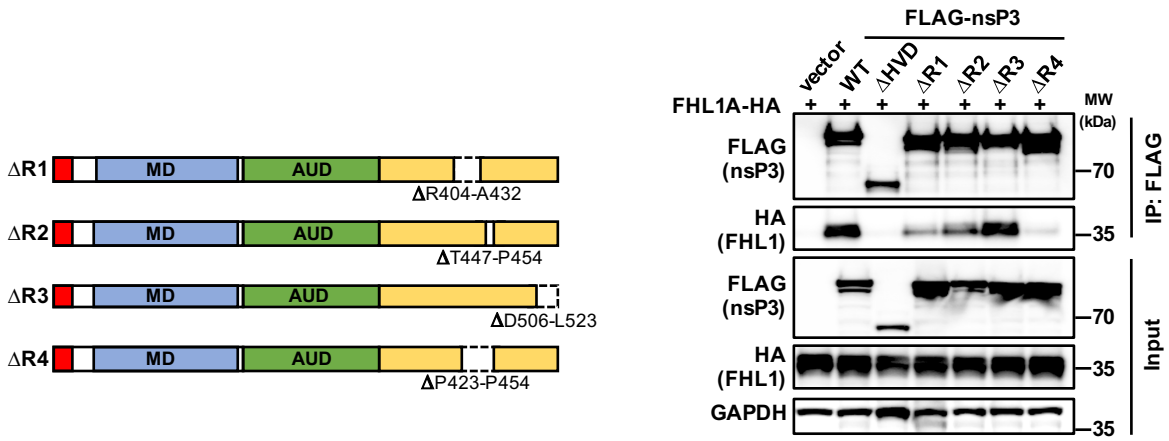

c

d

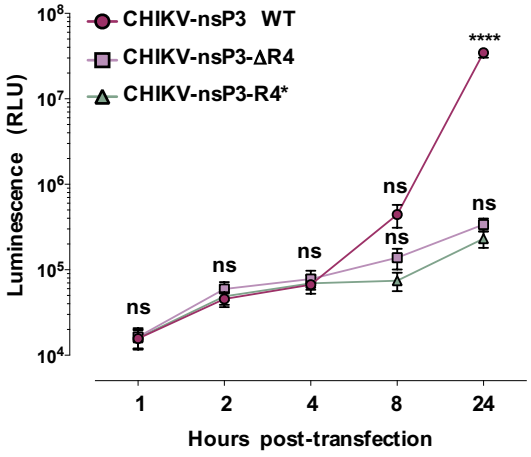

Extended Figure 7

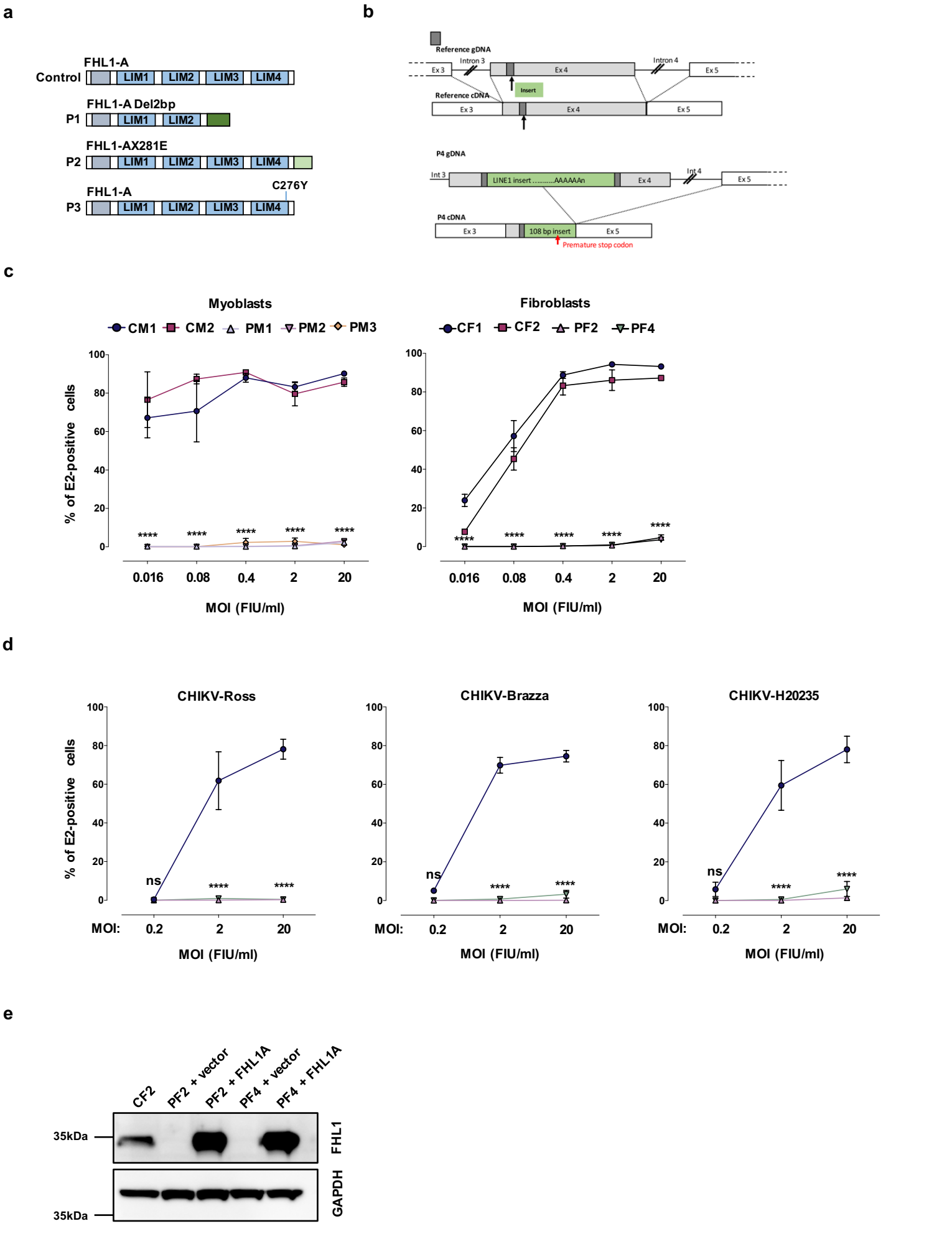

Extended Figure 8

a

```
Human FHL1A     ----------------MAEKFDCHYCRDPLQGKKYVQKDGHHCCLKCFDKFCANTCVECR  44
Murine FHL1     MASQRHSGPSSYKVGTMSEKFDCHYCRDPLQGKKYVQKDGRHCCLKCFDKFCANTCVDCR  60

Human FHL1A     KPIGADSKEVHYKNRFWHDTCFRCAKCLHPLANETFVAKDNKILCNKCTTREDSPKCKGC  104
Murine FHL1     KPISADAKEVHYKNRYWHDNCFRCAKCLHPLASETFVSKDGKILCNKCATREDSPRCKGC  120

Human FHL1A     FKAIVAGDQNVEYKGTVWHKDCFTCSNCKQVIGTGSFFPKGEDFYCVTCHETKFAKHCVK  164
Murine FHL1     FKAIVAGDQNVEYKGTVWHKDCFTCSNCKQVIGTGSFFPKGEDFYCVTCHETKFAKHCVK  180

Human FHL1A     CNKAITSGGITYQDQPWHADCFVCVTCSKKLAGQRFTAVEDQYYCVDCYKNFVAKKCAGC  224
Murine FHL1     CNKAITSGGITYQDQPWHAECFVCVTCSKKLAGQRFTAVEDQYYCVDCYKNFVAKKCAGC  240

Human FHL1A     KNPITGFGKGSSVVAYEGQSWHDYCFHCKKCSVNLANKRFVFHQEQVYCPDCAKKL      280
Murine FHL1     KNPITGFGKGSSVVAYEGQSWHDYCFHCKKCSVNLANKRFVFHNEQVYCPDCAKKL      297
```

b

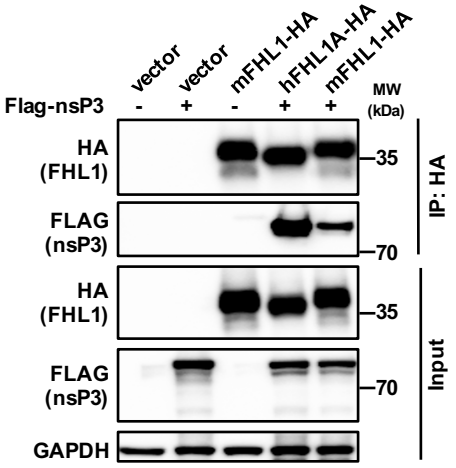

c

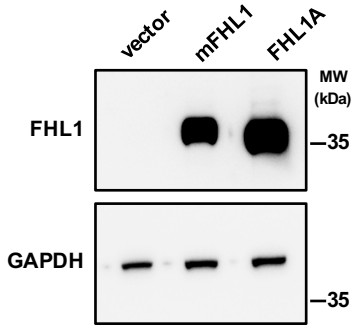

d

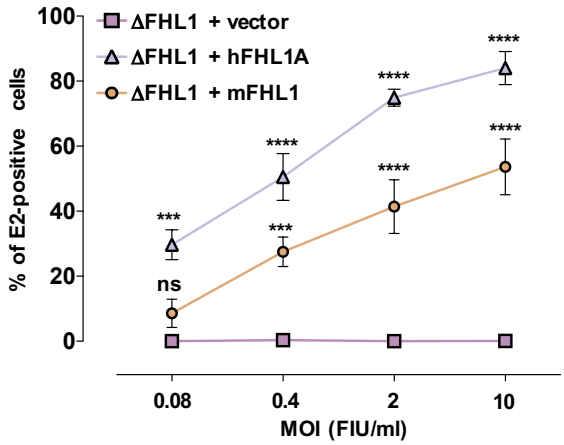

e

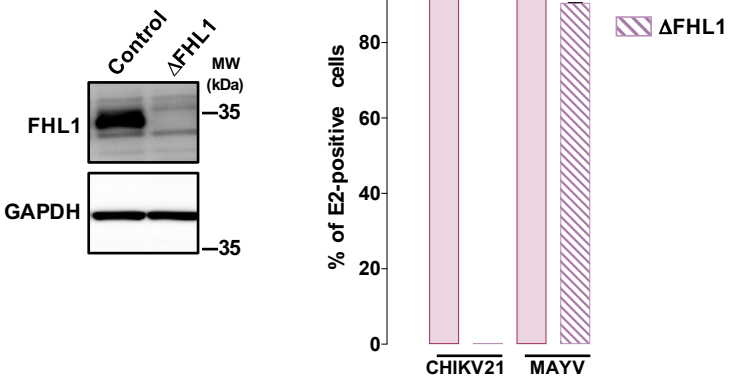

Extended Figure 9